SLAC–PUB–4604
April 1988
(E)

B–FACTORIES*

ELLIOTT D. BLOOM

Stanford Linear Accelerator Center
Stanford University, Stanford, CA 94309

ABSTRACT

We briefly review the physics of CP violation and the interest of studying this phenomenon in the B-meson system. The need for very large numbers of B-decays is shown, and a number of approaches for B-factories are compared. In particular, e^+e^- linear and circular colliders are discussed in some detail, with specific examples presented.

INTRODUCTION AND MOTIVATION

How to learn about the "next" energy scale has been a major occupation of particle physicists over the past few years. The SSC is one such obvious attempt, though perhaps not the most imaginative one (and certainly not the most economical). A lesson from history may have relevance to this question. The weak interaction has been very helpful in determining the electroweak scale, as well as determining the phenomenology of the electroweak interactions. Figure 1 reproduces one of the arguments, circa the early 1960's, which led to the conclusion that 100 GeV was the "natural" scale of the weak interaction. Extensive and frequently precision experiments at the available mass scale ($E^{\infty}_{cm} \sim 0.5$–30 GeV) over the next 20 years, using a variety of techniques, then led to a firm prediction of the W and Z masses, detailed knowledge of their decays, and the relatively economical machine designed to observe them at CERN in the 1980's. It is possible that history can repeat by using CP violation as a similar tool to explore the "next" mass scale.

The framework which we now consider CP violation is the KM matrix of the standard model with three quark-lepton generations. In this model, CP violation is the

* Work supported by the Department of Energy, contract DE–AC03–76SF00515.

Extended version of the Invited talk Presented at the 8th International Conference on High Energy Physics at Vanderbilt, Nashville, TN, October 8–10, 1987

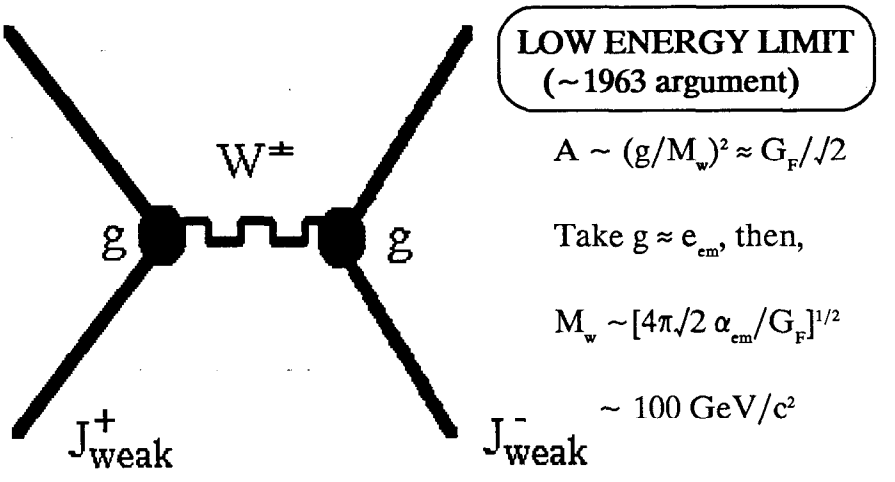

Figure 1. Lowest order weak interaction theory extrapolated in the early 1960's to estimate the mass scale of weak interactions.

result of the one irreducible phase in the KM matrix; indeed, three generations and the KM matrix were developed in large part to provide an explanation of CP violation in the early 1970's. At the present time, there seem to be two possibilities: the mass scale of CP violation is electroweak, or the mass scale is much larger. If the relevant mass scale which correctly describes CP violation is on the order of the present electroweak scale, one expects large CP violations in the B-meson system explainable in the context of the KM matrix. The ability to observe CP violation, if the standard model is correct, is considerably enhanced if the recent ARGUS collaboration results on B^0_d mixing are confirmed. ARGUS has obtained,[1]

$$X_d = \Delta M/\Gamma(B^0_d) = 0.78 \pm 0.16, \tag{1}$$

as compared to theoretical predictions in the range $X_d < 0.2$.[2]

The mixing is calculated using the real part of the box diagram of Fig. 2,[3]

$$\Delta M/\Gamma = (32\pi/3)\, \mathcal{R}e\{V_{tb}V_{td}^*\}/|V_{cb}|^2\, (B_B f_B^2 \eta_2 m_t^2/m_b^4). \tag{2}$$

The theoretical unknowns are the KM matrix elements, V_{tb} and V_{td}, the B-meson structure constant ($B_B^{1/2} f_B$), the QCD correction η_2, and the mass of the top quark, m_t. The large ARGUS mixing result and the B-lifetime measurements[4] (~ 10^{-12} sec.) imply a larger than predicted V_{td}, and smaller than predicted V_{cb}, respectively, as well as $m_t > 50$ GeV[5] (just about the mass lower limit measured by UA-1).[6]

Experimental estimates of ϵ and ϵ', from measurements of CP violation in the K^0 system,[7] where,

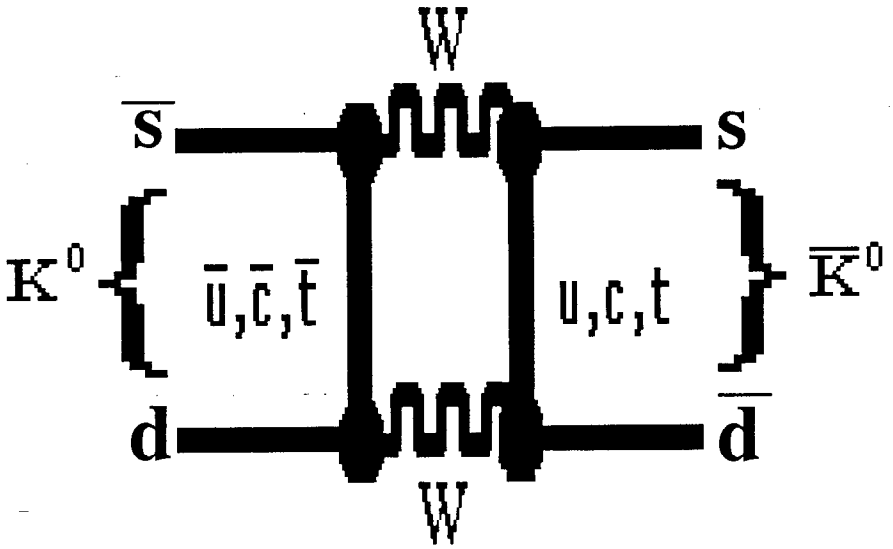

Figure 2. Second order box diagram used in the calculation of CP violation

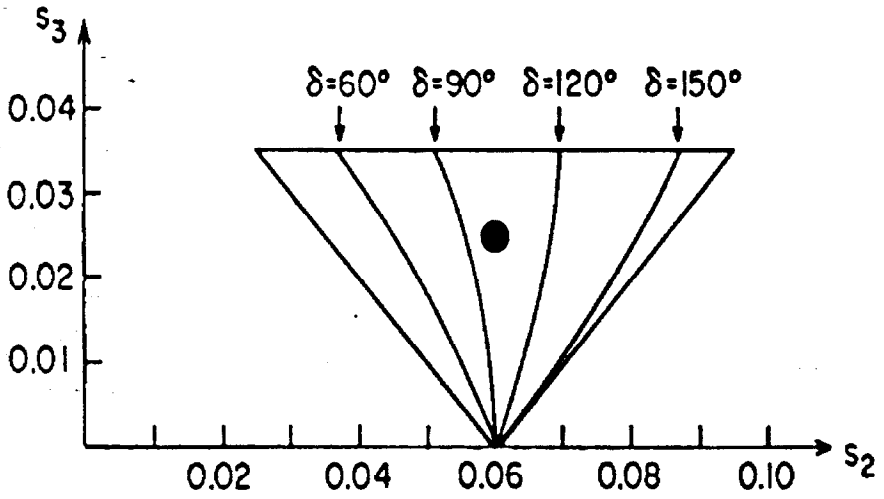

Figure 3. The allowed range of KM parameters as determined using b-quark lifetime and leptonic branching ratio. The "best" value is somewhat loosely chosen at the dot.

$$\eta_{+-} \equiv \text{amp}(K_L \to \pi^+\pi^-)/\text{amp}(K_S \to \pi^+\pi^-) = \epsilon+\epsilon' = 2.279(26) \times 10^{-3} e^{i\{44.6^\circ(1.2)\}}, \quad (3)$$

and,

$$\eta_{00} \equiv \text{amp}(K_L \to \pi^0\pi^0)/\text{amp}(K_S \to \pi^0\pi^0) = \epsilon-2\epsilon' = 2.29(4) \times 10^{-3} e^{i\{55^\circ(6)\}}, \quad (4)$$

then imply a large KM phase, $\delta \approx 100^\circ$.[8] Figure 3 shows the approximate values of s_2, s_3, and δ (KM matrix representation) inferred from the experiments.[8]

The large mixing, measured for B_d, and predicted for B_s, then implies an incredibly large CP violation in B-decays, on the order of 10%–50%.[5] A striking manifesta-

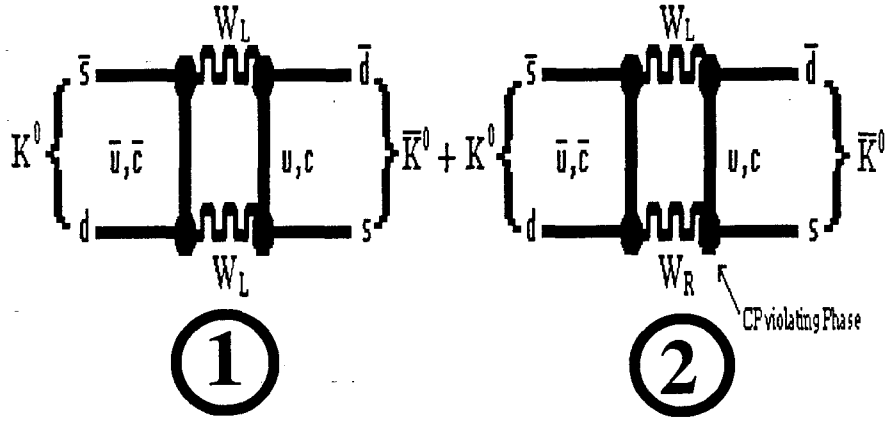

Figure 4. Box diagrams contributing to $\Delta M(K^0)$ and ϵ in left-right symmetric model. #2 contributes CP violating phase. Note that only two generations are involved in the model.

tion of CP violation is predicted to be a large difference in time evolution between initially B^0- and $\underline{B}^0$- mesons as they decay into particular final states. The reactions,

$$B^0_d \rightarrow \psi + K_s,\ B^0_d \rightarrow \psi + K^*, \text{ and, } B^0_s \rightarrow \psi + \phi, \tag{5}$$

look particularly accessible and promising for realizing a CP violation at this time.

What if the standard model is wrong? Then, there is probably a new mass scale and CP violation is its prophet. An example of such a model is the "minimal" left-right symmetric model involving a very heavy right-handed W.[9] Figure 4 shows the box diagrams relevant to this model. Assume that box 1 ≡ I, is relatively real, and that the entire CP violation in the K^0 system is due to box 2. Note that only two generations are included in the calculation, and thus we are effectively assuming that KM contributes nothing , or is irrelevant to CP violation ($\delta = 0$). In addition, we assume equal left- and right-handed Cabbibo angles. It can be shown,[9]

$$\text{box 2} = I \times [M(W_L)M(W_R)]^2 \times \underline{430} \times e^{i\varphi}\ , \tag{6}$$

where $M(W_{L,R})$ are the left- and right-handed W masses, respectively, $\underline{430}$ is a numerical factor which depends on the detailed structure of the theory, and φ is a CP violating phase induced by right-handed W exchange.

Assuming the entire CP violating effect is due to the diagrams of Fig. 4, we obtain, by comparing to experiment,

$$\Delta M_{LRS}(K^0) = \mathcal{R}e\{\text{box 2}\} = I \times [M(W_L)/M(W_R)]^2 \times 430 \times \cos\vartheta \leq \text{box 1} \tag{7}$$

$$\epsilon_{LRS}(K^0) = \mathcal{I}m\{\text{box 2}\} = [M(W_L)/M(W_R)]^2 \times 430(2\sqrt{2}) \times \sin\vartheta = 2 \times 10^{-3}\ . \tag{8}$$

These conditions imply that, 2 TeV $\leq W_R \leq$ 20 TeV.[9] In this case, CP violation in the B-system would be comparable to that in the K-system as the B-mass is still very small compared to $M(W_R)$. Very high precision CP violation experiments would then be needed in the B-system, as they are now needed in the K-system, to explore the source of the violation.

Both scenarios above promise many fruitful years of physics to come from a careful and systematic study of the B-system, if a sufficient number of B-decays are available. This last point, however, presents a severe challenge to the experimentalist.

WHERE TO "B"

The question of which B-meson sources, coupled with which detection techniques, looms as the major challenges in the future of B-meson studies.[10] There are two general areas of possibilities, proton machines and e^+e^- colliders. I will briefly discuss both sets of possibilities and then reflect in more detail on e^+e^- colliders, which is my area of specialization. Details for the proton machine option are given in Ref. 11.

Protons or Electrons

High energy proton machines, both fixed target and colliders, presently have some advantages as compared to e^+e^- colliders. First and most importantly, there exists the potential to produce very large numbers of B-mesons per unit running time. As Table 1 shows, up to 10^9 B's might be produced per day of running at the SSC, with lesser amounts from presently available machines. In addition, decay lengths for B's of a few mm may allow measurement of decay vertices with relative ease if radiation problems can be overcome. However, as is outlined in Table 1, these potential advantages are presently all but neutralized by a number of disadvantages. Although $\sigma_{tot} \sim 50$ mb, $\sigma(b\underline{b})/\sigma_{tot}$ is very small and thus the $b\underline{b}$ events are very difficult to extract with reasonable efficiency (even in Monte Carlo land). The trigger will be crucial here.[11] In addition, large multiplicities generated from the $b\underline{b}$ part of the event, coupled with many additional particles not associated with the $b\underline{b}$, exacerbate the problem of B–finding. Finally, the question of radiation damage from high doses near the target (or IP for colliders) presents a severe technological challenge.

Presently, conceived advantages and disadvantages for e^+e^- colliders are essentially orthogonal to those for proton machines. Although detection of B's is not simple here, experience has shown that the $\sigma(b\underline{b})/\sigma_{tot} \sim$ 0.1–.25 makes the problem rather

Table 1. Comparison of Hadronic Experiments

	TeV II Few Years	TeV II Improved	TeV Coll Few Years	TeV Coll Improved	SSC
E_{cm}(GcV)	40	40	2,000	2,000	40,000
$\sigma(b\bar{b})/\sigma_{tot}$	10^{-6}	10^{-6}	10^{-4}	10^{-4}	10^{-3}
$\mathcal{L}_{day}(pb^{-1})$*	3	30	.03	.3	limited by rate
Interactions 200 days	10^{13}	10^{14}	10^{12}	10^{13}	10^{14}
#BB/200 days	10^{7}	10^{8}	3×10^{7}	10^{9}	10^{11}
$\gamma\beta c\upsilon$ (mm)	7	7	2	2	3
$<n_{ch}>_{detector}$	8	8	100	100	50
Solid angle	0.2π	0.2π	$\sim 4\pi$	$\sim 4\pi$	$\sim\pi$

*Approximate Lumi limit producing 10^7 interactions/sec max. in some cases.

straightforward, and new detectors presently being built at Cornell, LEP, and SLAC will improve matters considerably. As is shown in Table 2, a small beam pipe radius is projected for a number of machines allowing improved lifetime measurements and flavor tagging. However, **the** question at e^+e^- colliders is rate. Figure 5 and Table 2 illustrate the problem. Even at the peak of the Z^0, where $\sigma_{b\bar{b}} \sim 6$ nb, rate is severely limiting. The problem is luminosity, or the lack thereof, for presently available or building e^+e^- colliders. It seems clear that if CP violation is to be explored by e^+e^- collider experiments, factors of 100–1000 in luminosity are needed over presently operating machines depending on E_{cm} and machine design, i.e., symmetric or nonsymmetric beam energies. Table 2 shows projected operating luminosities for a number of machines. Some of these machines are well along, while others are just at the conceptual stage. Through state-of-the-art and beyond, none of the machines in the table have the integrated luminosity to do anything but scratch the region of interesting limits on CP violation in the B-system.

Energy and Kinematics

Not only is the question of $\mathcal{L}$ vs σ_{tot}, i.e., production rate, a crucial issue for e^+e^- colliders, E_{cm} and movement of the center-of-mass are also important. The latter points relate to the measurement of CP violation though the spectacular signature of unequal partial widths, i.e., decay length vs time for certain combinations of final

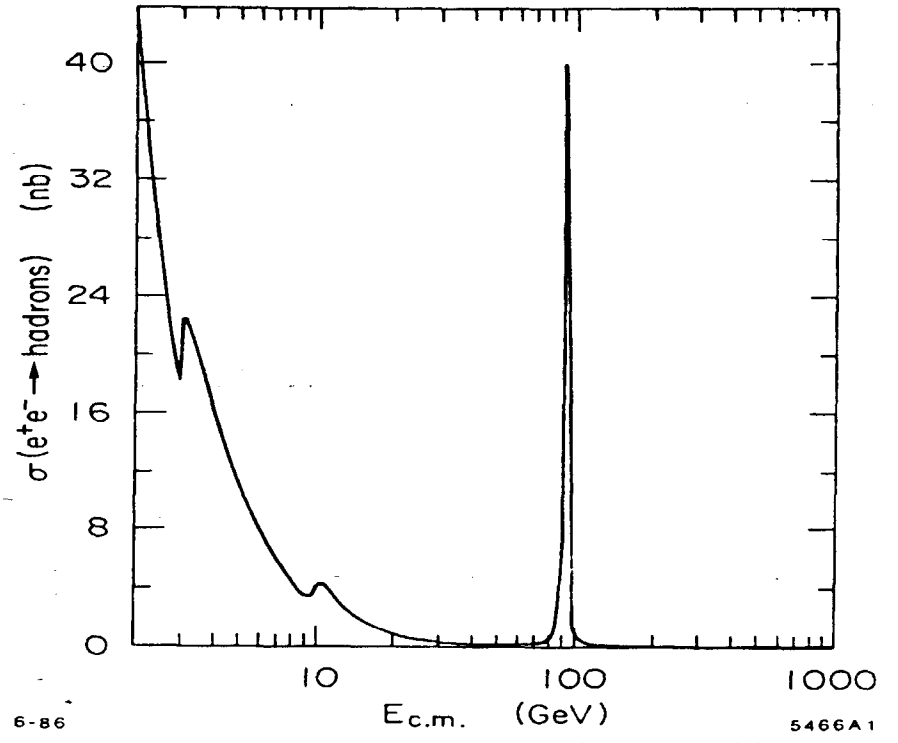

Figure 5. Approximate σ_{tot} vs E_{cm} for e^+e^- collisions.

Table 2. e^+e^- collider parameters

	CESR (1990's)	SIN* (1995 ?)	SBF# (1995 ?)	SLC (1990's)	LEP (1990's)	Lin. Coll. (2000 ?)
E_{cm}(GeV)	10 (4S)	10 (4S)	10–26	93 (Z^0)	93 (Z^0)	10–20
$\sigma(b\bar{b})/\sigma_{tot}$	0.25	0.25	0.1–0.25	0.15	0.15	0.1–0.25
σ_{tot}(nb)	3.9	3.9	0.05–1.0	40	40	1.0–3.9
$\mathcal{L}_{day}(pb^{-1})$	10	30	180(E_{Max})	0.2+	0.6	45–450+
#B$\bar{B}$/200 days	2×10^6	6×10^6	$\geq 1.6 \times 10^6$	2×10^5	6×10^5	10^7
$\gamma\beta c\tau$(mm)$_{Lund}$	0.01	0.01	0.01–0.5	2.4	2.4	.25–.5
$R_{beampipe}$(cm)	2–6	2–6	2–3.5	1–3	6–8	1–3
$\langle n_{ch} \rangle_{detector}$	6	6	6–10	20	20	6–10

* New proposal for a e^+e^- storage ring collider optimized for $\Upsilon(4S)$.

\# Conceptual design for a major upgrade to PEP, the Stanford Beauty Factory (see later Sections of this report).

\+ For linear colliders $\langle L \rangle = L_{peak}/2$, for storage rings $\langle L \rangle = L_{peak}/3$.

states for B^0 vs $\underline{B}^0$. For example, this phenomenon is predicted to occur for a CP self-conjugate decay mode, f, common to B^0 and $\underline{B}^0$,[12] and yields disparate time dependent partial widths for B^0 and $[\underline{B}^0]$ given by,

$$\Gamma\,(B^0[\underline{B}^0](t) \rightarrow f[\underline{f}]) \propto e^{-\Gamma t}\{1+\cos\Delta mt) \times |\rho_f|^2[1] + (1-\cos\Delta mt) \times 1[|\rho_f|^2] \\ -[+](2\,\sin\Delta mt) \times \Im m((p/q)\rho_f)\}, \qquad (9)$$

where, $\rho_f = A(B^0 \rightarrow f)/A\,(\underline{B}^0 \rightarrow f)$, $p/q = (1+\epsilon)/(1-\epsilon)$, and the authors of Ref. 12 have set $\Delta\Gamma = 0$, and $|p|^2 = |q|^2$ for simplicity, and with the expectation that these approximations are accurate. An example of such a decay is $B^0 \rightarrow \psi K^0_s$, though the size of the CP violation in each particular case is a matter of some conjecture.[5]

Figure 6 shows examples of events from the decay,[13]

$$B^0 \rightarrow D^0\pi^+\pi^- \rightarrow K^+\pi^-\pi^+\pi^- \ , \qquad (10)$$

and its charge conjugate as seen at different E_{cm} and for the case of, $E_{beam} = 12.5$ GeV on $E_{beam} = 2.0$ GeV with $E_{cm} = 10$ GeV, i.e., asymmetric $\Upsilon(4S)$ production. As the figure qualitatively demonstrates, either symmetric production well into the continuum or asymmetric production at the $\Upsilon(4S)$ (or other resonances with low Q, e.g., the $\Upsilon(5S)$ for B^0_s $\underline{B}^0_s$ production) is needed to enable observation of the spectacular CP violating effects associated with decay length interference.

In addition to enabling the start of the search for CP violation in the B-system, some of the machines whose properties are outlined in Table 2 have impressive yields of other heavy flavors. The latter is shown in Table 3, where large yields of τ's and charm are shown for the $\Upsilon(4S)$ and continuum machines. As the branching ratio to $\tau\underline{\tau}$ from the Z^0 is only a few percent, machines presently planned for the Z^0 are not competitive for τ physics.

The efficiency of identification of $B\underline{B}$ pairs and the correct assignment of decay products to the B and $\underline{B}$ are of paramount importance in CP violation experiments. Much of the present deficit in rate at e^+e^- colliders might be made up by clever detection and tagging strategies. The problems at a stationary $\Upsilon(4S)$ are formidable in this respect; however, it is not so clear at this time whether asymmetric production at lower masses or symmetric production in the continuum optimize efficiencies at significantly different levels. Considerably more work with data and Monte Carlo has to be done for a rational decision to be made. Some work has been done com-

paring stationary Υ(4S) production to that in the continuum, and a summary is shown in Figs. 7–10.[14]

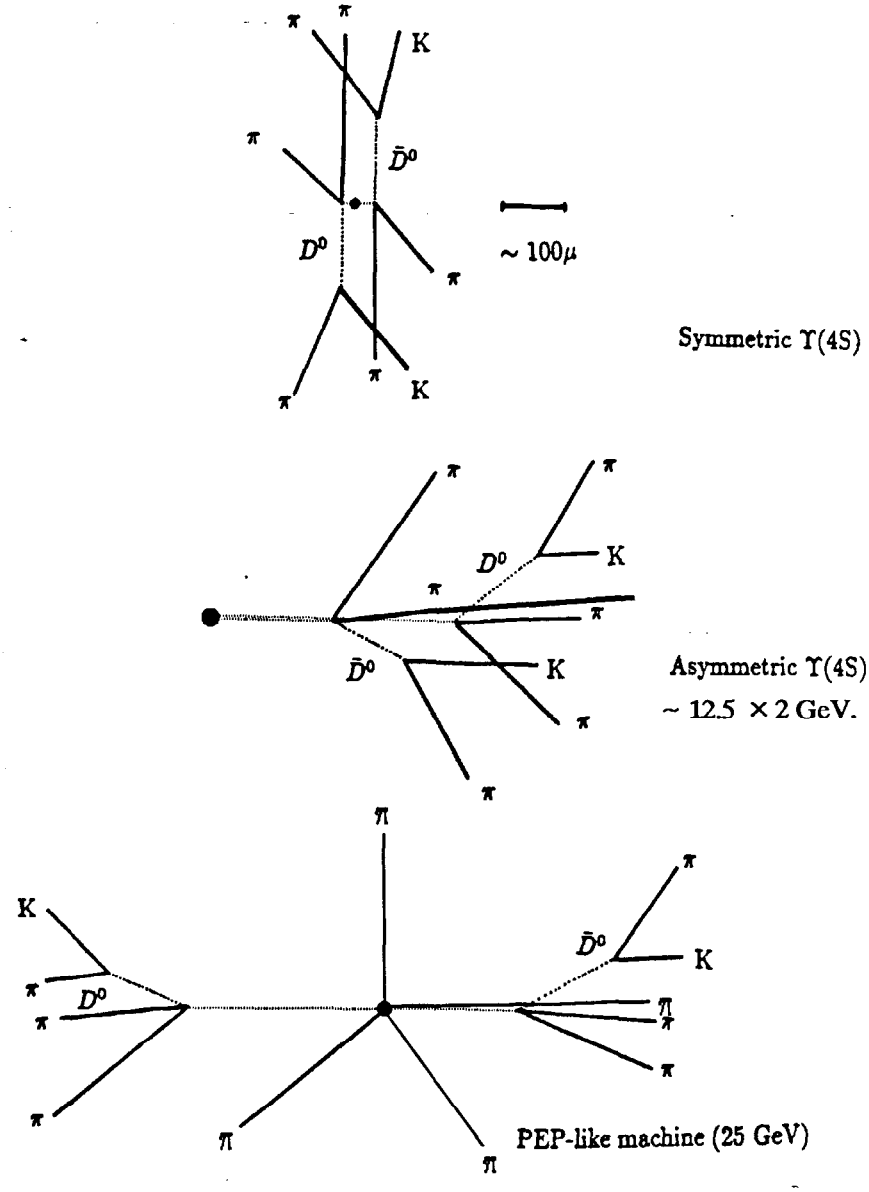

Figure 6. Simulations of a prototypical B$\underline{\text{B}}$-decay as seen in different machines, both symmetric and asymmetric.

Table 3. Heavy flavor yields from e^+e^- colliders

	CESR (1990's)	SIN (1995?)	SBF (1995?)	SLC (1990's)	LEP (1990's)	Lin. Coll. (2000 ?)
# $B\underline{B}$/200 days	2×10^6	6×10^6	1.6×10^6	2×10^5	6×10^5	10^7
# $C\underline{C}$/200 days	2×10^6	6×10^6	6×10^6	1.6×10^6	5×10^6	4×10^7
# $\tau\underline{\tau}$/200 days	1.7×10^6	5×10^6	4.5×10^6	4.8×10^4	1.5×10^5	3×10^7
Note: $f_\tau = 0.02$ @ Z^0, $f_\tau = 0.21$ in the continuum.						

Some of the figures were generated from Ref. 14 which used an early version of the Lund Monte Carlo[15] for E_{cm} between the $\Upsilon(4S)$ and 60 GeV; a smooth extrapolation to the Z^0 at E_{cm} of 92 GeV was then made (shown as dashed lines in two of the figures). As the work of Ref. 14 used the Lund symmetric B-fragmentation function, the results sensitive to fragmention function were redone for the entire energy range with a more accurate model. [16] Figure 7 defines the general topology of the $B\underline{B}$ events with most of the B jet and $\underline{B}$ jet on opposite sides of the IP and a few extra π's produced at the event vertex. Figure 8a shows n_{ch}, the charged multiplicity in the $\underline{B}$ jet summed with the prompt charged particles, vs E_{cm}. Figure 8b shows $n_c(>1\text{GeV})$, the number of charged particle with momentum > 1 GeV/c, vs E_{cm}. Figure 9 shows $<\beta\gamma>$ for the B's and the average impact parameter, <d>, for decay particles with $|\mathbf{p}|$ > 1 GeV/c, vs E_{cm}. Though $<\beta\gamma>$ grows linearly with E_{cm}, $<\delta>$ increases much more slowly for E_{cm} > 20 GeV. Note that a "typical" e^+e^- storage ring beam size is about $20\times350\ \mu$ (vertical × horizontal) with "mini-β," while the SLC beam size will be $\sim 2\times2\ \mu$.

Figures 10a–c continue with a more quantitative description of the general topology of the $B\underline{B}$ events. Figure 10a shows the distribution in rapidity with respect to the sphericity axis for $B\underline{B}$ events with E_{cm} = 29 GeV. The solid line is the distribution for all charged particles, the dashed line for the charged particles from a B-decay in each event. Figure 10b shows $<n_{na}>$, the mean number of charged particles not associated with the B-decay, but within the B-decay rapidity region. Figure 10c shows the fraction of tracks with momentum > 1 GeV/c emitted into the hemisphere of the opposite $\underline{B}$. Clearly, as E_{cm} increases to about 25 GeV a rapid improvement in the isolation of the B and $\underline{B}$ jets occurs with only a mild increase of multi-

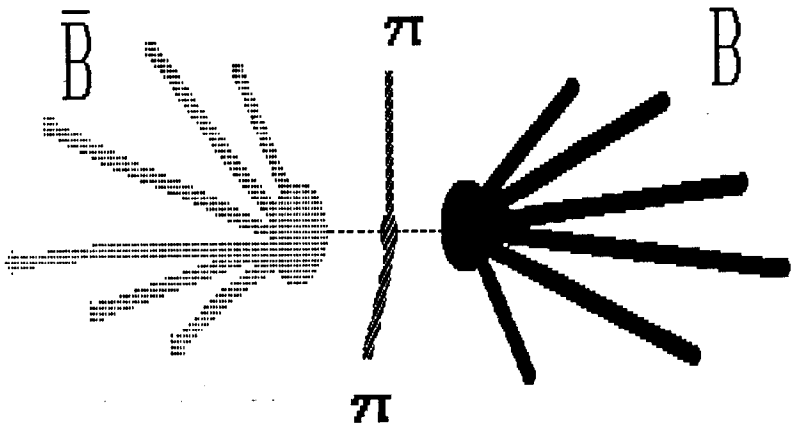

Figure 7. Representation of a B$\underline{\text{B}}$ event at $E_{cm} \sim 25$ GeV. The π's at the e^+e^- vertex come from the central rapidity region and can be removed by a simple rapidity cut. The vertices associated with the B- and $\underline{\text{B}}$-decays are then revealed.

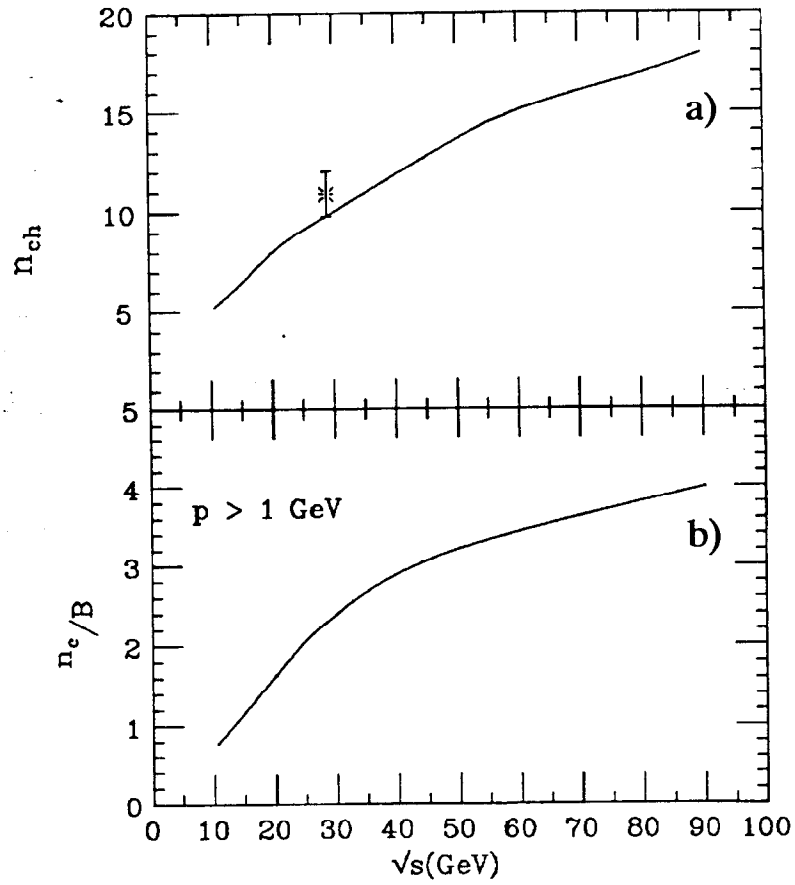

Figure 8. a) n_{ch}, the charged multiplicity in the $\underline{\text{B}}$ jet summed with the prompt charged π's vs E_{cm}. The solid line is from the Lund M.C.,[16] the data point is from the TPC/ 2γ collaboration.[17] b) n_c, the number of charged particles with $|\mathbf{p}| > 1$ GeV/c, vs E_{cm}. The solid line is from the Lund M.C.[16]

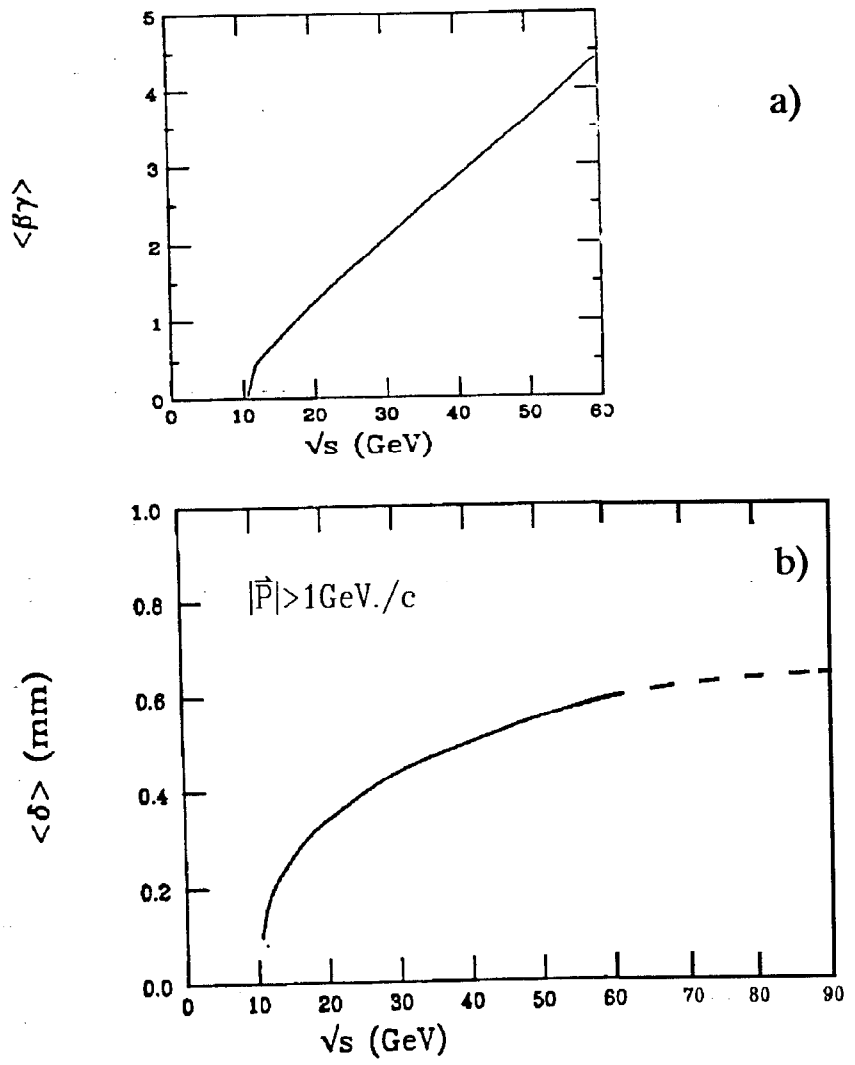

Figure 9. a) $<\beta\gamma>$ for the B's, vs. E_{cm}. b) $<\delta>$, the average impact parameter for particles decaying from B's with momentum greater than 1 GeV/c, vs E_{cm}. The solid lines are from Ref. 14, dashed line is an extrapolation.

plicity. In addition, $<\delta>$ increases dramatically over this range. However, as one proceeds to higher E_{cm}, isolation and $<\delta>$ improvement saturate while multiplicity continues to increase. It thus seems that for symmetric colliders, E_{cm} in the range 20–30 GeV yield the best topological features for a broad range of B physics which involves B and $\underline{B}$ separation and lifetime determination, features important to CP violation measurements. As mentioned previously, asymmetric and symmetric collider configurations are still in need of a detailed comparison.

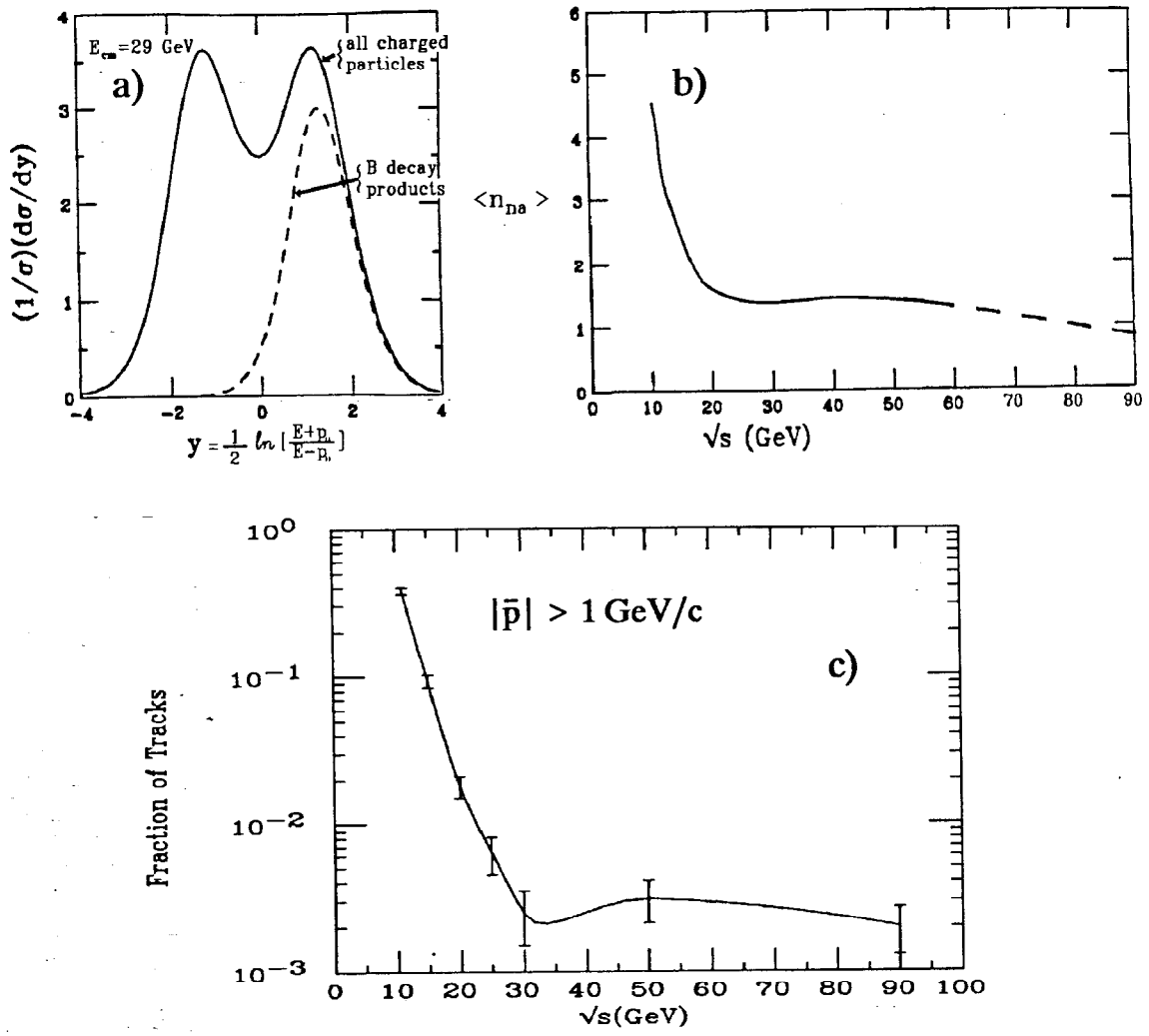

Figure 10. a) Distribution in rapidity, y, with respect to the sphericity axis for B$\underline{\text{B}}$ events with E_{cm} = 29 GeV. The solid line is the distribution for all charged particles, the dashed line for the charged particles from a B-decay in each event.[14] b) $<n_{na}>$, the mean number of charged particles not associated with the B-decay, but in the B-decay y region.[14] The dashed part of the curve is extrapolated. c) "Fraction of Tracks" with $|\mathbf{p}| > 1$ GeV/c emitted into the hemisphere of the opposite $\underline{\text{B}}$.[16] The errors on the points indicate the statistical uncertainty of the Monte Carlo.

The ability to verticize a B$\underline{\text{B}}$ event is a crucial aspect of CP violation measurements. Much work has yet to be done before such capability is available, with the development of two-dimensional and low mass vertex tracking within 1–2 cm of the IP essentially a prerequisite. Vertex tracker (VT) resolutions of ~20 μ in both dimensions will be required, as well as material thickness of less than ~0.5% of a radiation length for the VT and beam pipe combination. Note that for the case of a 500

MeV/c particle, 0.5% rl, $\theta_z \sim 90^\circ$ @ 1 cm from the IP, the position error from multiple scattering is $\Delta x \sim 20\ \mu$ at the IP. Higher momentum for the particles determining the vertex will be helpful, and so strategies which tag on high energy leptons, as that in Ref. 18, may be important.

Figure 11 shows such a B$\underline{\text{B}}$ event where one B decays to $\psi(l^+l^-)$ + $K^*(K\pi)$, and the other B is tagged by a lepton with $E_l > 1$ GeV (perhaps with a K depending on efficiency).

As the B-meson inclusive decay to ψ is large, at about 1.25%, the decay of a B to lepton pairs from a ψ is about 0.2%. Given the results of Ref. 18, and considering a Stanford Beauty Factory (SBF) at design luminosity (see Table 1), and a new detector optimized to this type of physics (including VT), one estimates that in a year of data taking (200 days): about 6000 $\psi \rightarrow l^+l^-$ are produced, half of which are detected; about 350 $B^0_d \rightarrow \psi(l^+l^-)K\pi$ are fully reconstructed (including vertex); taking $B^0_s/B^0_d \sim 0.5$, about 150 $B^0_s \rightarrow \psi(l^+l^-)\ \phi(KK)$ are fully reconstructed; and finally, assuming a 0.1% branching ratio, one expects 200 fully reconstructed $B^0_d \rightarrow \psi(l^+l^-)K_s$-decays. If the opposite B($\underline{\text{B}}$) semi-inclusive tag (including vertex) has a 50% efficiency, a CP

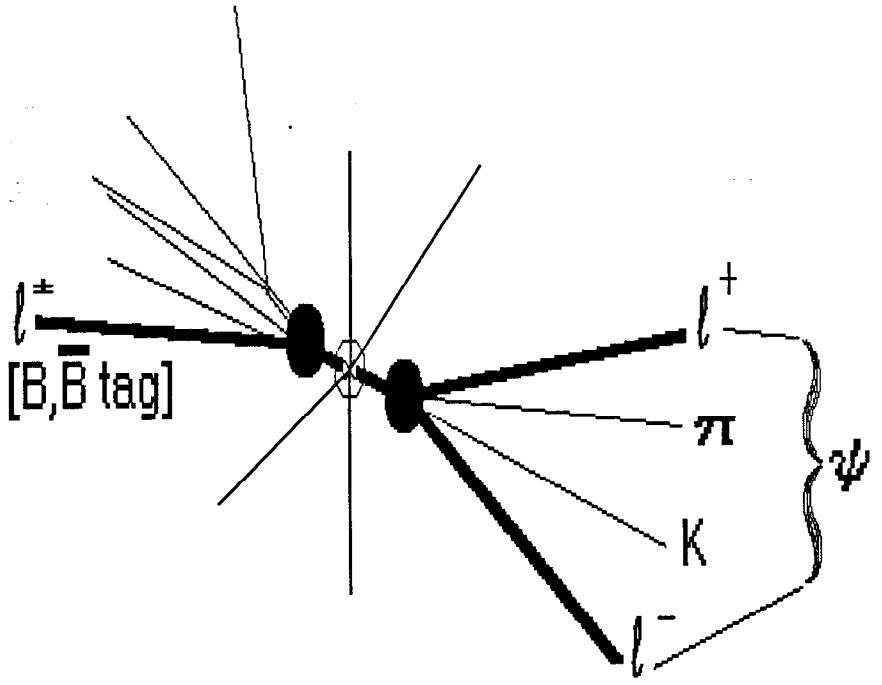

Figure 11. B$\underline{\text{B}}$ event with one B vertex tagged by ψ decay to l^+l^- and the other B identified as B or $\underline{\text{B}}$ via a lepton tag. A CP violation measurement is possible using time dependence of difference of decay vertices for B vs $\underline{\text{B}}$.

violation measurement may be possible using the time dependence of decay for B vs $\underline{B}$. Given present day speculations on the size of the CP violation in these channels ($\sim 10\%$–50%),[5] about a five-year run could be sufficient to see an effect. Note that the detector alluded to above is well beyond what is now available.

e^+e^- MACHINE CONCEPTS

In this report I will discuss two general types of approaches to B-factories, linear colliders and storage ring colliders. The section on linear colliders stresses design basics and illustrates these with three examples of "high tech" design concepts. In my opinion, storage ring colliders presently offer a more rapid path to progress in B--meson measurements, and perhaps the fastest path to the first measurements of CP violation in the B-system. I thus have put more emphasis on the circular machines, and the section on circular machines is thus considerably more detailed and discusses examples of machines that either exist, or are rather conventional in concept.

Linear Colliders

The basic theoretical expressions for luminosity, $\mathcal{L}$, disruption parameter, D, and corresponding luminosity enhancement, H_D, and beamstrahlung for $e^\pm$ linear colliders have been discussed before.[19] I will review them briefly before presenting a few machine design concepts.

The luminosity can be written in practical units in terms of the beam power, P_b, the disruption parameter, $D(=D_y)$, the pinch enhancement factor, H_D, the bunch length, σ_z, and the beam aspect ratio, $R = \sigma_x/\sigma_y \geq 1$, as,

$$\mathcal{L}(cm^{-2}sec^{-1}) = 3 \times 10^{31} \{DH_D P_b(MW)/\sigma_z(mm)\} \times \{(1+R)/2R\} \quad . \tag{11}$$

In more basic terms,

$$\mathcal{L}(10^{32}cm^{-2}sec^{-1}) = 8 \times 10^{-6} \{[N(10^{10})]^2 \, f_b(Hz) \, H_D/[4\pi A(\mu m^2)]\} \quad , \tag{12}$$

where, N is the number of $e^\pm$ per bunch, f_b is the bunch collision rate — usually the linac repetition rate, and $A = \sigma_x\sigma_y$ is the beam area. A is given in terms of the invariant emittance and the beta functions at the collision point as,

$$A = (\epsilon_{nx}\epsilon_{ny}\beta^*_x\beta^*_y)^{1/2}/\gamma \quad , \tag{13}$$

where, $\gamma = E_b/m_e$, E_b is the beam energy and m_e is the mass of the electron.

The disruption parameter plays an important role in the design of linear colliders which are pushing the limits of luminosity, as are the B-factory designs discussed

below. H_D, the pinch enhancement factor which is a function of D, is used in these designs to gain an order of magnitude or more in luminosity. The disruption parameter is given by,

$$D_y = 14.4\{N(10^{10})\ \sigma_z(\text{mm})/[E_b(\text{GeV})A(\mu\text{m}^2)]\} \times \{2R/(1+R)\} \ . \qquad (14)$$

The round beam pinch enhancement factor, H_{D0}, has been calculated by a number of groups and somewhat different values have resulted.[20] Figure 12 shows the results of two of the calculations, and they differ substantially for large D. Indeed, the qualitative behavior for H_{D0} for $D > 10$ is very different in the two calculations. The more recent calculations also find a dependence on σ_z/β^*_z, with about a 30% decrease seen in H_{D0} as σ_z/β^*_z increases from 0.1 to 0.4. H_D for any aspect ratio can be expressed in terms of the round beam enhancement factor H_{D0} as follows,

$$H_D(R,D_y) = RH_{D0}/[1 + (R-1)H_{D0}^{1/2}] \ , \qquad (15)$$

where, H_{D0} is evaluated at D(round beam) = D_y.

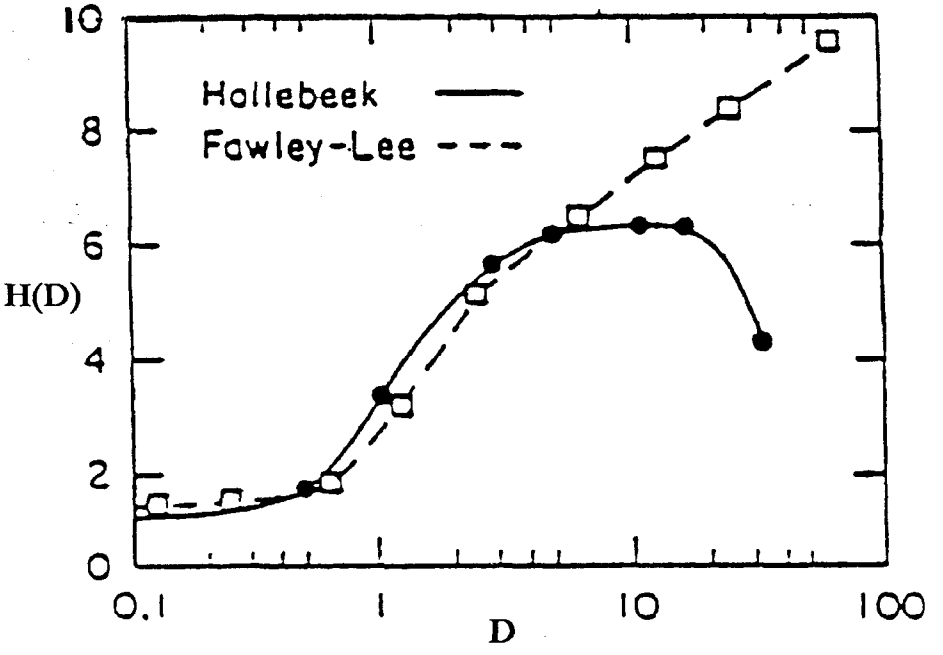

Figure 12. Two calculations of H(D) vs D.[20] The later calculation of Fawley and Lee indicates no limit to beam pinch enchancement, in contrast to the earlier calculation of Hollebeek.

The maximum beam disruption angles at the collision point are also an important aspect of the design. The spent beams have to pass through the near quads before being dumped, and also experimental backgrounds have to be shielded against. A reasonable approximation to the maximum disruption angle is given by,

$$\theta_{Dx}(\text{mr}) \approx \theta_{Dy}(\text{mr}) \sim 30\, N(10^{10})/\{E_b(\text{GeV})[\sigma_x(\mu\text{m}) + \sigma_y(\mu\text{m})]\}. \qquad (16)$$

Another source of experimental background is synchrotron radiation. In addition to the normal sources associated with the focusing of the beams in the near quads, high luminosity linear colliders have the added source of beamstrahlung which originates in the beam-beam interaction at the collision point. In addition to the potential experimental background which comes from the radiated photons from beamstrahlung, the beam energy spread is made broader. The latter effect can be quite important if one is considering a $\Upsilon(4S)$ machine, and so designs frequently have $\Upsilon(4S)$ and continuum running parameters which can differ by over an order of magnitude in projected luminosity. The qualitative character of the beamstrahlung depends on the value of a scaling parameter $\Upsilon \equiv 2\omega_c/3E_b$, where ω_c is the critical energy for classical synchrotron radiation. For gaussian bunches Υ can be written as,

$$\Upsilon = 3.1 \times 10^{-3}\{E_b(\text{GeV})N\mathcal{L}(10^{32})/[\sigma_z(\text{mm})f_b(\text{Hz})]\} \times \{2[1+(R-1)\sqrt{H_{D0}}]/[2+(R-1)\sqrt{H_{D0}}]\}\ , \qquad (17)$$

where the formula above is approximately correct for gaussian bunches of any aspect ratio and disruption parameter. There are two limiting beamstrahlung regimes: the classical where $\Upsilon << 1$, ($\omega_c << E_b$), and the quantum regime were $\Upsilon >> 1$, ($\omega_c >> E_b$). B-factory designs will generally be in the classical regime where the mean energy radiated due to beamstrahlung is given by,

$$\langle\delta_{cl}\rangle = 0.120\{E_b(\text{GeV})\mathcal{L}(10^{32})/[\sigma_z(\text{mm})\, f_b(\text{Hz})]\} \times \{4[1 + (R-1)\sqrt{H_{D0}}]/[2 + (R-1)\sqrt{H_{D0}}]^2\}\ , \qquad (18)$$

and the average number of beamstrahlung photons per collision is given by,

$$\langle N_\gamma\rangle = 2.2\ \langle\delta_{cl}\rangle\ \Upsilon^{-1}\ . \qquad (19)$$

The rms center of mass energy spread of the machine is then given by the following simple expression,

$$\sigma_W/W = 0.32[1+10/\langle N_\gamma\rangle]^{1/2}\langle\delta_{cl}\rangle\ . \qquad (20)$$

Of course there are many other aspects to the design of a linear collider beside the

theoretical formulae presented above. For more detailed information I highly recommend the papers of Ref. 19. For example, one of the most severe contemporary problems is how to make the very large number of "cold" positrons needed for such high luminosity machines. However, this brief introduction gives sufficient background to understand the list of machine parameters typically presented in design studies.

A number of conceptual designs have been advanced for linear collider B-factories. Table 4 shows the parameters of a design using a superconducting linac structure as proposed by Amaldi and Coignet,[21] an asymmetric design powered by a parallel driving beam (two-beam accelerator) proposed by Wurtele and Sessler,[22] and a very high gradient (200 MeV/m), high frequency (10 kHz) concept proposed by Cline.[23] All of these ideas have many "high tech" elements incorporated into the designs. To bring any of these concepts to a real machine is likely to take a very considerable development.

Table 4. Parameters for a few linear collider T(4S) factory designs.

	Ref. 21	Ref. 22	Ref. 23
E_b^+(GeV	5.3	12.0	5.3
E_b^-(GeV)	5.3	2.3	5.3
$\mathcal{L}(10^{33}cm^{-2}sec^{-1})$	1.0	1.0	2.4
$e^{\pm}$/bunch(10^{10})	5.0	2.0	5.0
Bunch freq (kHz)	12.0	70.0	10.0
σ_z(mm)	1.3	$0.6^+/0.1^-$	0.1
$\sigma_{radial}(\mu m)$	1.1	1.0	0.2
$D/H)_{Hollebeek}$	16.0/6	1.35/5	3.0/6
$<P_b>$(MW)	0.53	3.1	0.44
δ_{cl}	4.5×10^{-4}	3.0×10^{-4}	4.0×10^{-3}

Storage Ring Colliders

The results of a previous section indicates that a good machine design for the observation of CP violation in B-meson decay is a very high luminosity e^+e^- symmetric storage ring operating at E_{cm} ~ 20–25 GeV. As SLAC has a machine of the appropriate radius, it is worthwhile to consider some improvements to the present

HiLum PEP machine which might possibly achieve the desired level of performance. In the process, we will explore many details of e^+e^- storage ring design. The two ideas I will discuss involve multiple bunch machines, much like the SIN proposal in spirit. Indeed, the general design criteria used are very similar to those used by K. Wille for the SIN proposal;[24] this is not an accident.

There are a few basic criteria. The storage ring should have many bunches; the beam should fill the available physical aperture at all operating energies; there should be only one IR, or two at the most, where the beams collide; there should be a small β_y at the IR, β^*_y. These considerations result from the following formula,

$$\mathcal{L} \propto (nf_u) \times \epsilon_{x0} \times (\Delta\nu)^2/\beta^*_y \ , \tag{20}$$

where, nf_u is the number of bunches, n, times the revolution frequency, f_u, (nf_u is independent of machine size for the same inter-bunch spacing), ϵ_{x0} is the natural horizontal emittance of the beam, and $\Delta\nu$ is the linear tune shift.

Assuming that the single bunch characteristics transfer to the multi-bunch case (no easy feat), the reason for the first factor is evident. More bunches means more luminosity (maybe even linearly with the number of bunches). Multi-bunching has been made to work by the CESR group at Cornell.[25] The second factor, ϵ_{x0}, should be made as large as possible with cost being the limiting consideration. The larger ϵ_{x0}, the larger the vacuum pipe, magnet apertures, and other apertures have to be. Also, for machines where rf power is a limitation, larger ϵ_{x0} typically means more power. For machines which will operate at E_b appreciably less than E^{max}_b, wiggler magnets should be used to fill the available physical aperture at the lower E_b.[26] The question of maximum $\Delta\nu$, the third factor, is related to the number of IR's, and will be discussed below. Finally, the influence of β^*_y is clear.

The question of maximal $\Delta\nu$ is important for achieving high $\mathcal{L}$. Figure 13 shows accumulated machine data plotted,[27] $\Delta\nu/\gamma(\times 10^7)$ vs $1/(n\rho)$, where, $\gamma = E_b/m_e$, and ρ is the machine bending radius. The plot shows data from many machines, and from the old (6 IR) PEP with 1 and 3 bunches per beam. These data imply (fitted line) that $\Delta\nu$ increases, $\propto(n\rho)^{-1/2}$, as the amount of energy radiated between collisions increases, $\propto(n\rho)^{-1}$, all other variables equal (e.g., E_b). That is, as one increases the damping time between collisions, the attainable $\Delta\nu$ increases. There are those that believe there is also theoretical evidence for this scaling law as well.[28] Such a scaling law

favors machines with fewer IR's, with one IR being optimum. The newly completed HiLum PEP has but one IR and will yield an important test of the scaling law with $\Delta\nu$ ~ 0.08 expected at E_b = 14.5 GeV. This value is shown on the figure as, n = 3, 1 IR, HiLum PEP (projected). The scaling law also favors the use of wiggler magnets that do not only fill the aperture of the storage ring, but also excite maximum damping consistent with available rf power. The installation of such wigglers at PEP, motivated by their utility for the synchrotron radiation program, has been previously suggested.[29]

The design numbers that appear later in this report have been obtained from the following formulae which work reasonably well for existing machines, [24]

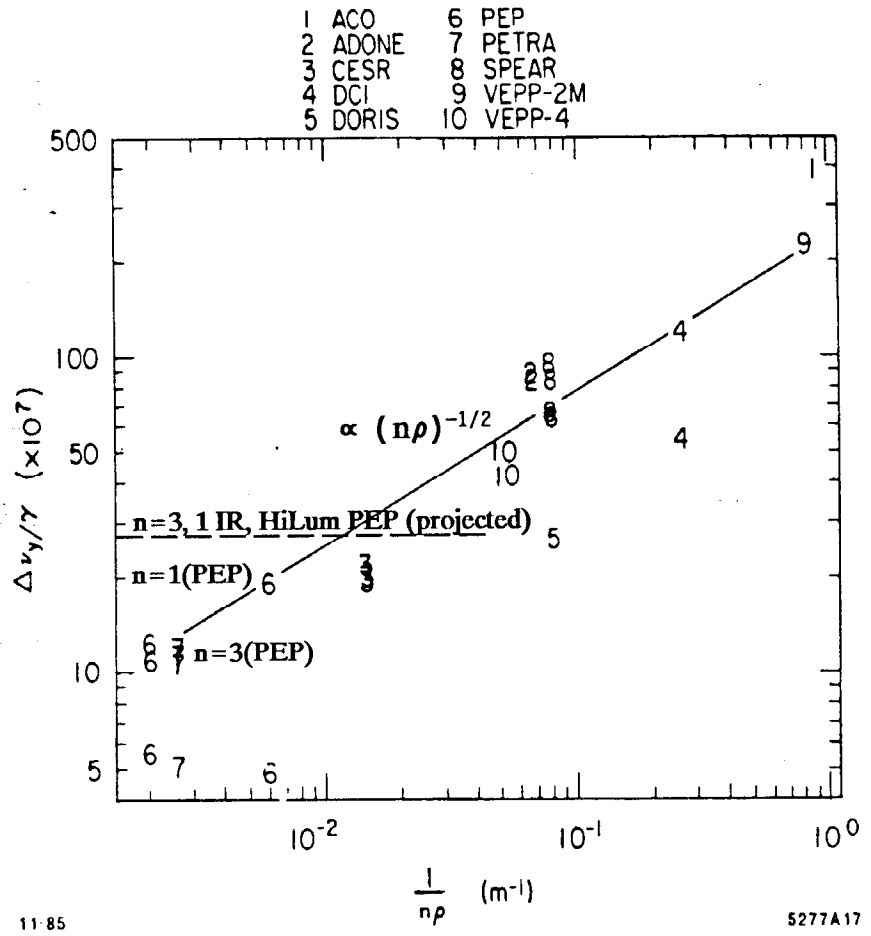

Figure 13. Empirical scaling of the maximum vertical linear tune shifts with machine bend radius, ρ, and number of bunches per beam, n.[27] In particular, values are indicated for old PEP for n = 1 and n = 3, as well as the projected value for HiLum PEP (and SBF). The projection is made using the fit to the data shown in the figure as a solid line.

$$(I^{bunch})_{max} = 698.5\ f_u E_b \epsilon_{x0} \Delta\nu \quad ,$$

and,

$$\mathcal{L}_{peak} = 1.51 \times 10^{32} [n f_u E_b^2 (1+\kappa^2)^2\ \epsilon_{x0} (\Delta\nu)^2 / \beta^*_y] \quad , \tag{22}$$

where, E_b is the beam energy, and κ is the horizontal-vertical beam coupling, $\kappa = (\epsilon_y / \epsilon_x)^{1/2} = (\beta^*_y / \beta^*_x)^{1/2}$. Note that in the above formulae $\Delta\nu_x = \Delta\nu_y = \Delta\nu$ is assumed. For many existing machines "optimal" coupling is $\kappa \sim 0.2$. We also assume that ϵ_{xo} "fills the aperture," i.e., ϵ_{xo} is constant, as a function of E_b; this was not assumed in Ref. 24. Filling the machine aperture at $E_b < E^{Max}_b$ can be done with wiggler magnets placed at proper locations in the machine lattice.[26]

Figure 14 shows a schematic layout of a two ring machine with one IR. Following the design of K. Wille,[24] a zero crossing angle is taken at the IP. In order to accomplish a zero crossing geometry a combination of electric or time varying magnetic, and static magnetic guide fields are needed. Static magnetic guide fields alone bend the e^- and e^+ beam in the same direction, as the e^- and e^+ are moving in opposite directions (this is why single ring storage rings work). Figure 15a shows the geometry needed and illustrates the principle of operation of an rf separator.[30] Figure 15b[24] shows a possible

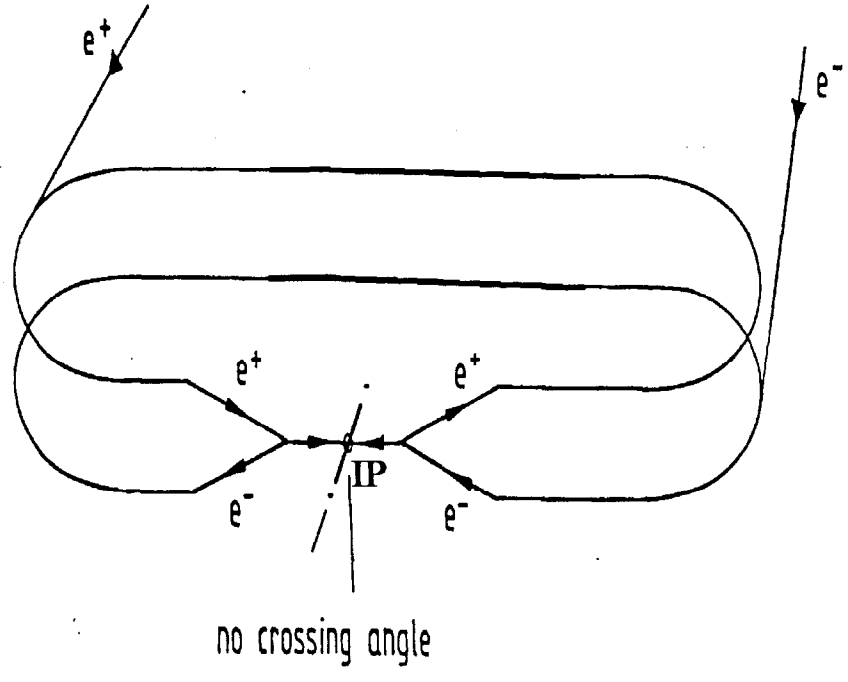

Figure 14. A schematic layout of a two ring e^+e^- storage ring with one IR This concept has a zero crossing angle at the one IR.

(21)

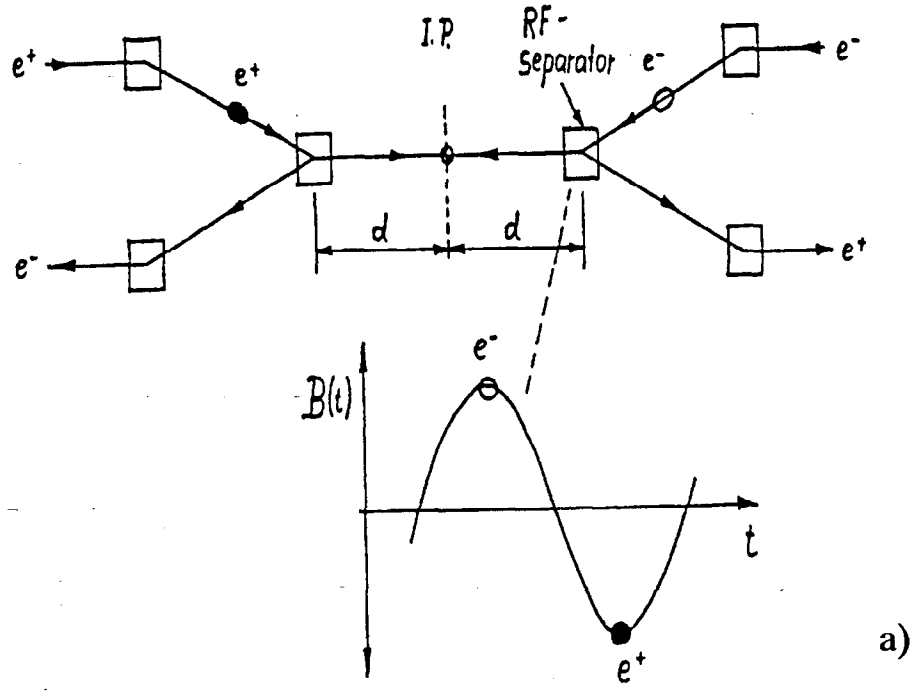

a)

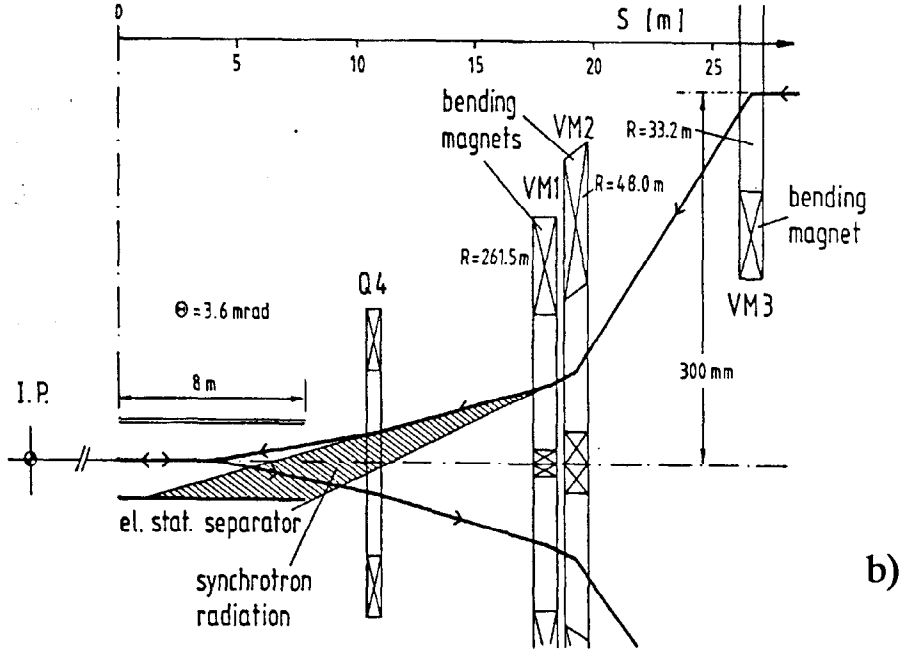

b)

Figure 15. a) Geometry needed for a zero angle crossing IR. Also shown is the principle of operation of an rf magnetic separator. b) A more detailed geometry from the SIN proposal for a zero angle crossing IR using electrostatic separator plates.

geometry using electrostatic separator plates. As is discussed by Wille,[30] both techniques need further development with a decision for one scheme or the other based on the results of experiments.

Figure 16 shows a plan view of the proposed SIN B-Meson factory.[24] The facility includes $e^{\pm}$ sources, an accumulator ring, a booster synchrotron allowing injection to

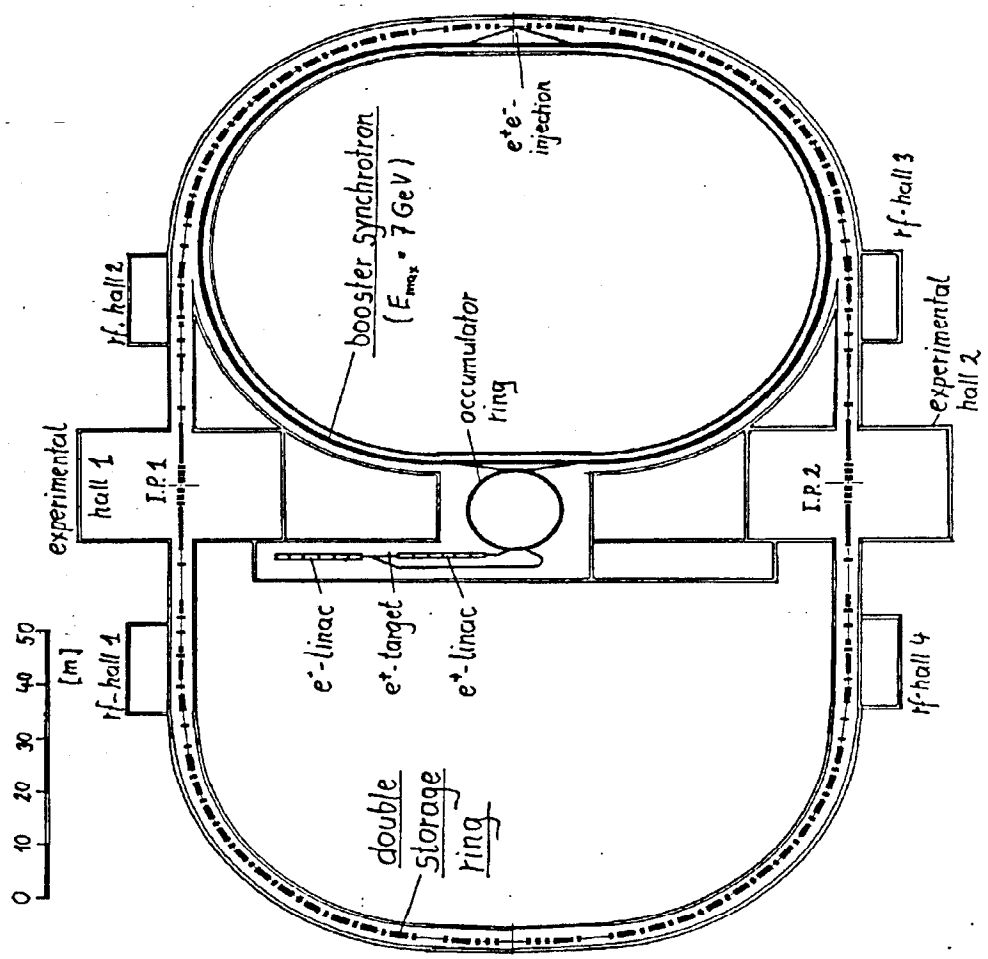

Figure 16. The proposed SIN facility.[24] Included are an e^- linac, e^+ target and linac used to accelerate $e^{\pm}$ to an energy of about 200 MeV. The two beams are then accumulated and compressed in a damping ring or accumulator ring. A booster synchrotron is then needed to inject at energy to the main storage rings. Finally, a double ring storage ring with two IR's completes the facility. At least one totally new detector is also being proposed.

a maximum of 7 GeV, a double ring storage ring which is 520 m in circumference, and two experimental halls enclosing 2 IR's. This machine will be a symmetric collider intended for optimum operation at the T(4S). It will be a multiple bunch machine, ultimately operating with 12 bunches per beam (inter-bunch spacing of 43 m), with currents up to 0.75 A per beam.

SCALING THE SIN DESIGN TO A STANFORD BEAUTY FACTORY (SBF)

In order to scale this design to $E_{cm} \sim 25$ GeV, we will consider the major points mentioned in the section on storage ring colliders.

First, the number of bunches. A minimum bunch spacing of 20–40 m is dictated by the rise time of the feedback systems needed to control the multi-bunch instabilities, and the geometry of the IR. The collisions should be head-on to avoid the problems that DORIS I had. The long straight sections of HiLum PEP are particularly amenable to a double ring upgrade as there is considerable room for matching the arcs to the IR's. With a separation of 31 m, 70 bunches can be put uniformly in a double ring machine. In addition, the very long straight sections of 117 m, see Fig. 17, allow an initial phase of multi-bunching to be done without a double ring (SBF_0). For separation in the straight sections only (there is not enough aperture in the arcs) the present PEP ring can be used. This scheme allows 15 bunches per beam placed in three groups of five bunches with each bunch in a group separated by 20 m from the next. The single ring multi-bunch PEP, SBF_0, has about five times fewer bunches and thus five times lower $\mathcal{L}$ than a double ring; however, this scheme is relatively inexpensive to build, and could yield a factor of five in $\mathcal{L}$ over the present HiLum PEP.

Second, the aperture. The SIN machine[24] is planned to have quite a large emittance allowing $\epsilon_{x0} = 8.3 \times 10^{-7}$ m-rad. This is accomplished by keeping $\beta \leq 30$ m in the ring, rather than by having a larger than normal physical aperture. For the SBF calculations we will use the present HiLum PEP emittance, $\epsilon_{x0} = 1.2 \times 10^{-7}$ m-rad. Note that ϵ_{x0} is defined by $\sigma_x \approx \sqrt{(\epsilon_{x0}\beta_x)}$, $(\eta = 0)$. Wigglers are needed to bring beam size to the aperture limit at $E_b < 14.5$ GeV, and to assure the tune shift limit of the design. Figure 18 shows a schematic of a three pole wiggler with trim sections at either end which allow a match into the machine lattice.

The use of wiggler magnets has been extensively discussed in Refs. 26 and 29. I will review the basic principles of operation below. The increase in emittance, $\epsilon^{w}_{x0}/\epsilon_{x0}$, is

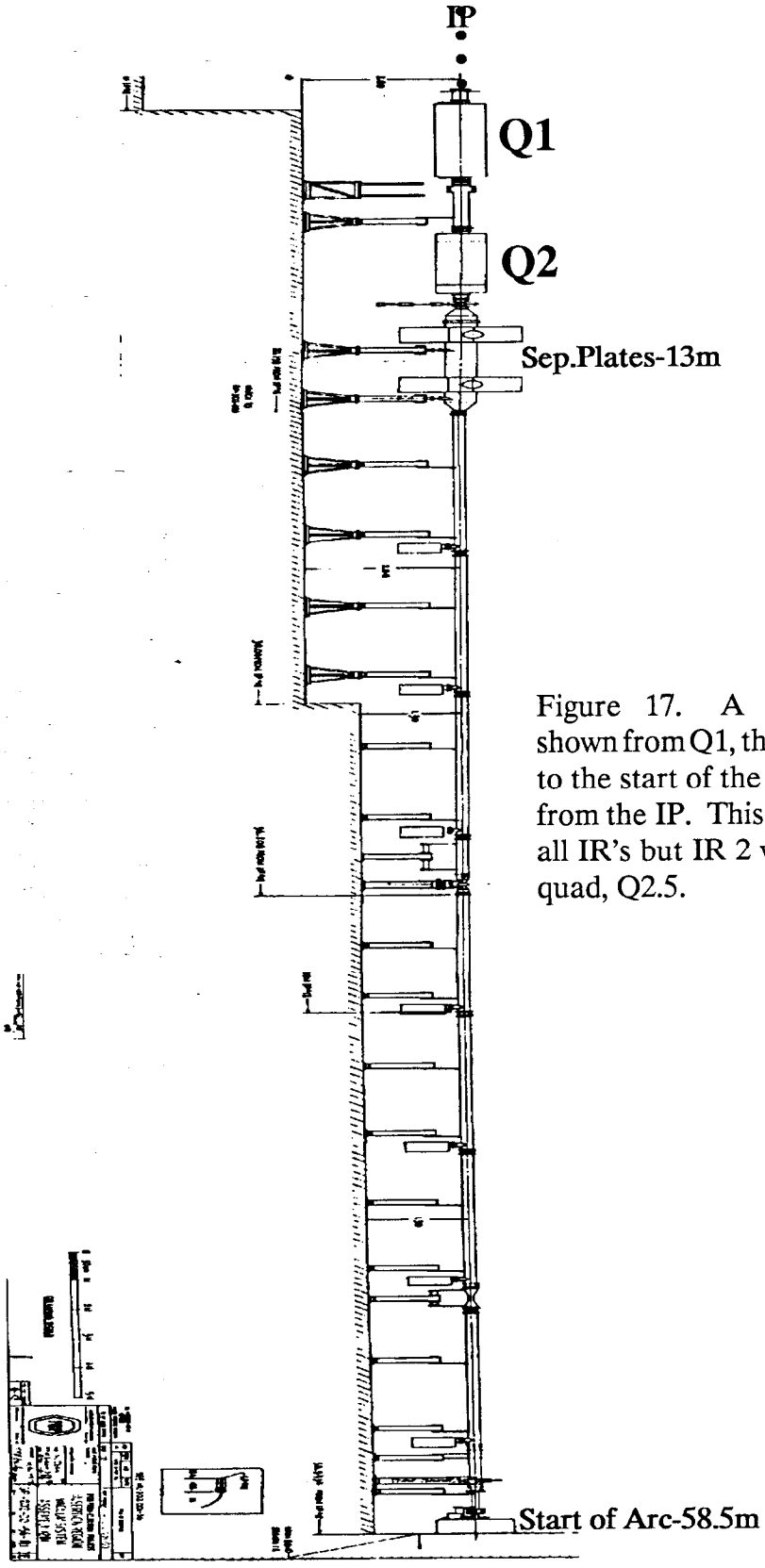

Figure 17. A PEP straight section shown from Q1, the first quad after the IP, to the start of the bending arcs at 58.5 m from the IP. This section corresponds to all IR's but IR 2 which has an addtional quad, Q2.5.

given by,

$$\epsilon^{w}_{x0}/\epsilon_{x0} \approx [1 + (<H_w>L_w/(<H_0>L_0)) \times (\rho_0/\rho_w)^3]/[1 + (\rho_0/\rho_w)^2] \quad , \tag{24}$$

where, ρ_0 is the main bend radius of the storage ring, ρ_w is the wiggler magnet bend radius, L_0 is the length of the machine bends, and L_w is the effective length of the wiggler. The H's are more complicated, with H_0 being a complex function of the machine lattice.[26] H_w is reasonably approximated by,

$$<H_w> \sim <\eta^2/\beta>_w \quad , \tag{25}$$

where the average is taken over the length of the wigglers. Note that for the old PEP, $<H_w>/<H_0> \sim 1$.

The stored beam's damping time is given by,

$$\tau_w/\tau_0 \sim [1+ (L_w/L_0) \times (\rho_0/\rho_w)^2]^{-1} \quad , \tag{26}$$

where, τ_0 is the damping time of the beam without wigglers. In order to damp the beam more quickly rf power is needed. The energy loss per turn, U0, increases as wiggler strength is increased, and,

$$U0_w/U0 = \tau_0/\tau_w \quad . \tag{27}$$

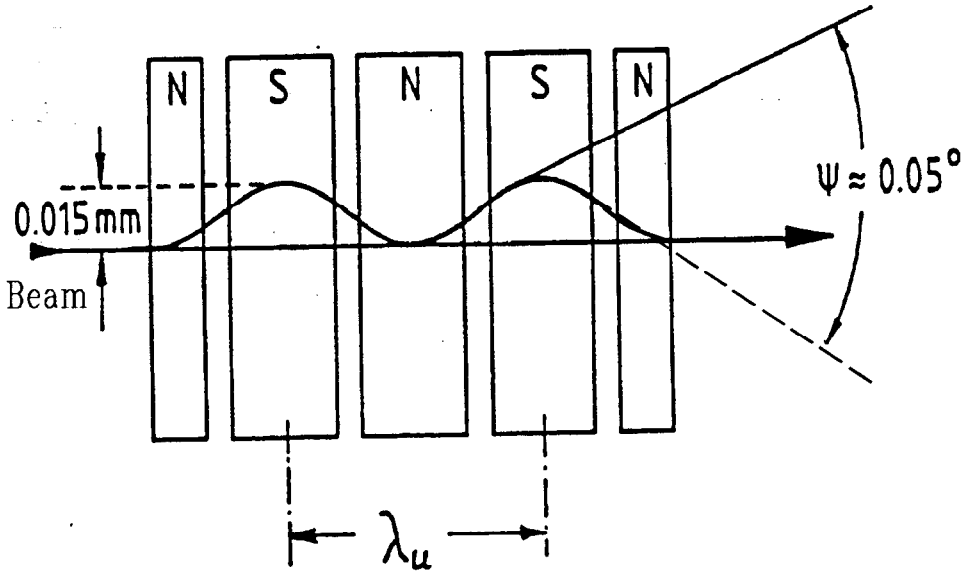

Figure 18. Schematic of a three pole wiggler magnet with trim magnets on either end to allow matching into the storage ring lattice. ψ is the maximum angle of bend of the beam as it wiggles through the magnets, and λ_μ is the wavelength of the "wiggle."

The above formulae show that by adjusting η and β at the wiggler location, one can tune the tradeoff between beam size and damping time over a wide range, however, at a cost of additional rf power.

Third, the tune maximum tune shift. As DORIS II has achieved $\Delta\nu_{max} \sim 0.025$, Wille[25] has been conservative in his design specs in specifying $\Delta\nu_{max} \sim 0.025$ as the initially achievable tune shift for the proposed SIN, which has features reminiscent of DORIS II. However, Wille projects that $\Delta\nu_{max} \sim 0.05$ will be possible eventually. PEP has achieved $\Delta\nu_{max} \sim 0.05$ in its old carnation and the scaling laws discussed in Section 3a imply that, using wigglers for $E_b < 14.5$ GeV, $\Delta\nu_{max} \sim 0.08$ will be possible for the SBF (and SBF_0).

Fourth, the β^*_y. Figure 19a shows the low beta insertion for the proposed SIN machine. This design is state-of-the art with two superconducting quads required (per side), and only 0.6 m between the face of the last superconducting quad and the IP. β^*_y is quite modest at three cm and cannot be made much smaller as dictated by the natural bunch length for storage rings with rf frequency in the 350–500M MHz range; β^*_y should be no smaller than $\sim 1.5 \times \sigma_z$. Figure 19b shows a possible IR arrangement for the SBF (and SBF_0). With the first major quads at 2.75 m, a three cm β^*_y is possible. In addition, a very smooth beam pipe, and minimal length of rf cavities are needed in all machines of this type due to the high currents and the possible effects of beam bunch lengthening.

Finally, superior injection is required so as to allow rapid filling of the storage ring. The stored current goals for the SIN proposal are, $I_{max} \sim 0.75$ A per beam, while for the full blown SBF concept $I_{max} \sim 0.85$ A per beam. In the case of the SBF, injection at 5×10^9 particles per pulse, at a 60 Hz injection rate, and with 50% capture efficiency will take ~ 4 min per beam. As the proposed SIN ring has a circumference which is about four times smaller, it would require about one min per beam with the same filling rate. For topping off (both machines will fill at energy without the need for ramping), divide the times by ~2. The SBF_0 would need about five times less time than the SBF, or about the same as the SIN proposal. DORIS II has actually achieved impressive filling rates, with topping off typically requiring only one or two minutes. Figure 20 shows a typical day's record when the system is fully operational. However, the three new machines discussed here have injection requirements which are an order of magnitude or more greater than DORIS II. Powerful injectors are required or much longer times will be taken for fills.

a) SIN

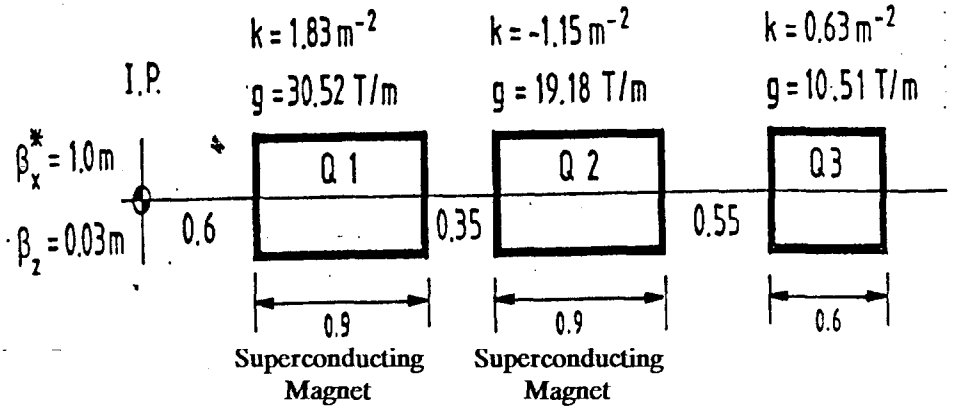

b) SBF

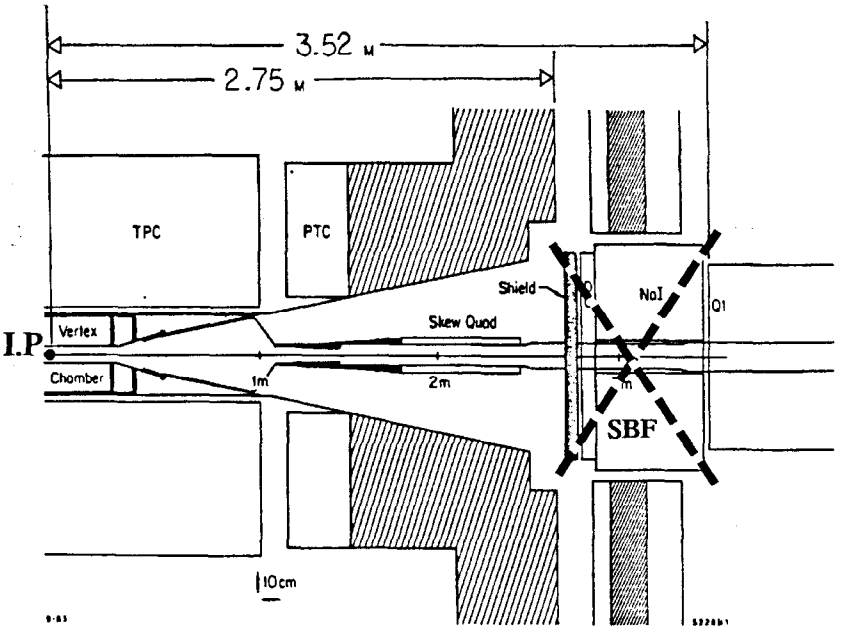

Figure 19. a) Preliminary design of the SIN IR.[19] This design requires two (pairs) of superconducting quads with the face of the nearest quad at 0.6m from the IP. b) Concept for the SBF IR. The first large quad is a standard PEP Q1 at a distance of 2.75 m from the IP. This should allow for β^*_y ~3 cm as is the case for SIN. The present TPC/2γ forward detector will have to be redesigned to accomodate the new Q1 location.

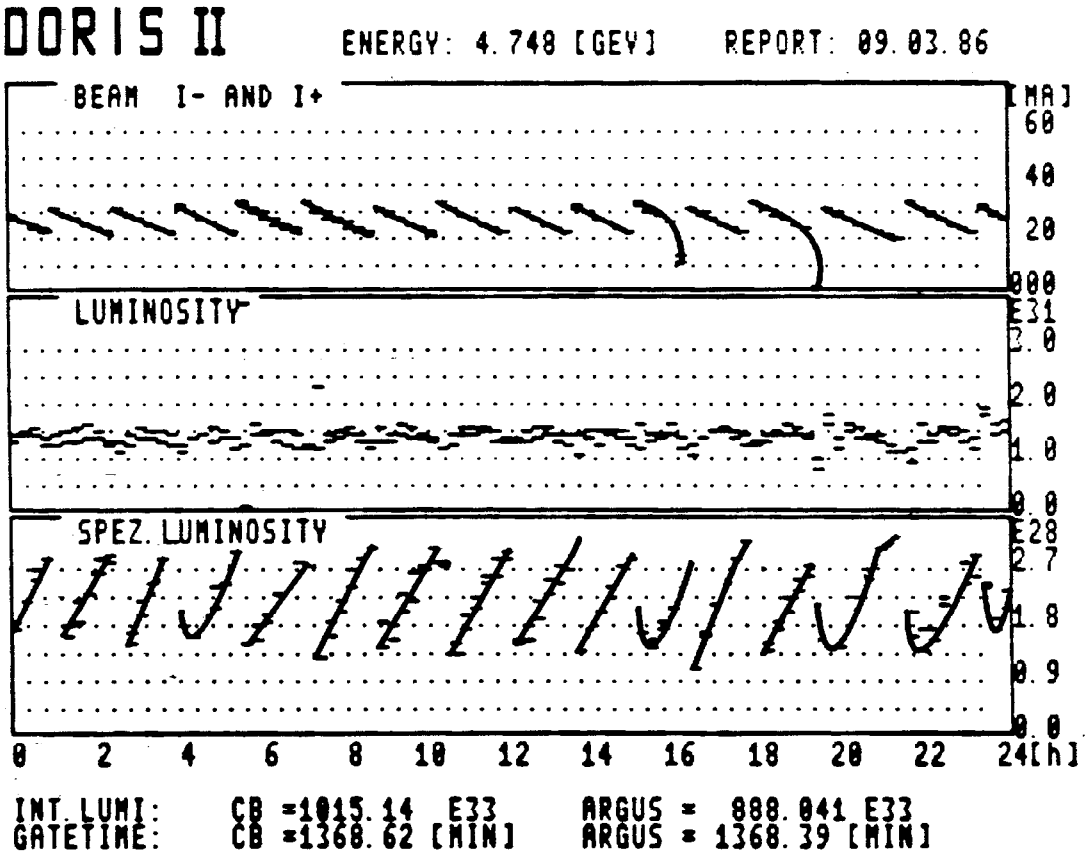

Figure 20. A typical day of injection at DORIS II when the injection system is fully operational. This quality of injection was not unusual after the initial bugs in the storage ring were found (took about 1.5 years of operational experience).

LUMINOSITY ESTIMATES

Figure 21 shows the design luminosity for the SIN proposal. Wille expects the luminosity to increase in stages as more is learned and improvements are made.[30] The bottom curve in the figure is expected within the first year of operation, with subsequently higher levels achieve as operating experience is gained. Finally, after some years of operation, $\mathcal{L}_{peak} \sim 3 \times 10^{33}$ cm^{-2}sec^{-1}, is projected at the Υ(4S).

The SBF can also be staged. Initially, the SBF_0 can be built, at modest cost, and operational experience with multi-bunch and high currents will be gained. If and when it appears possible and desirable to gain an additional factor of about five in luminos-

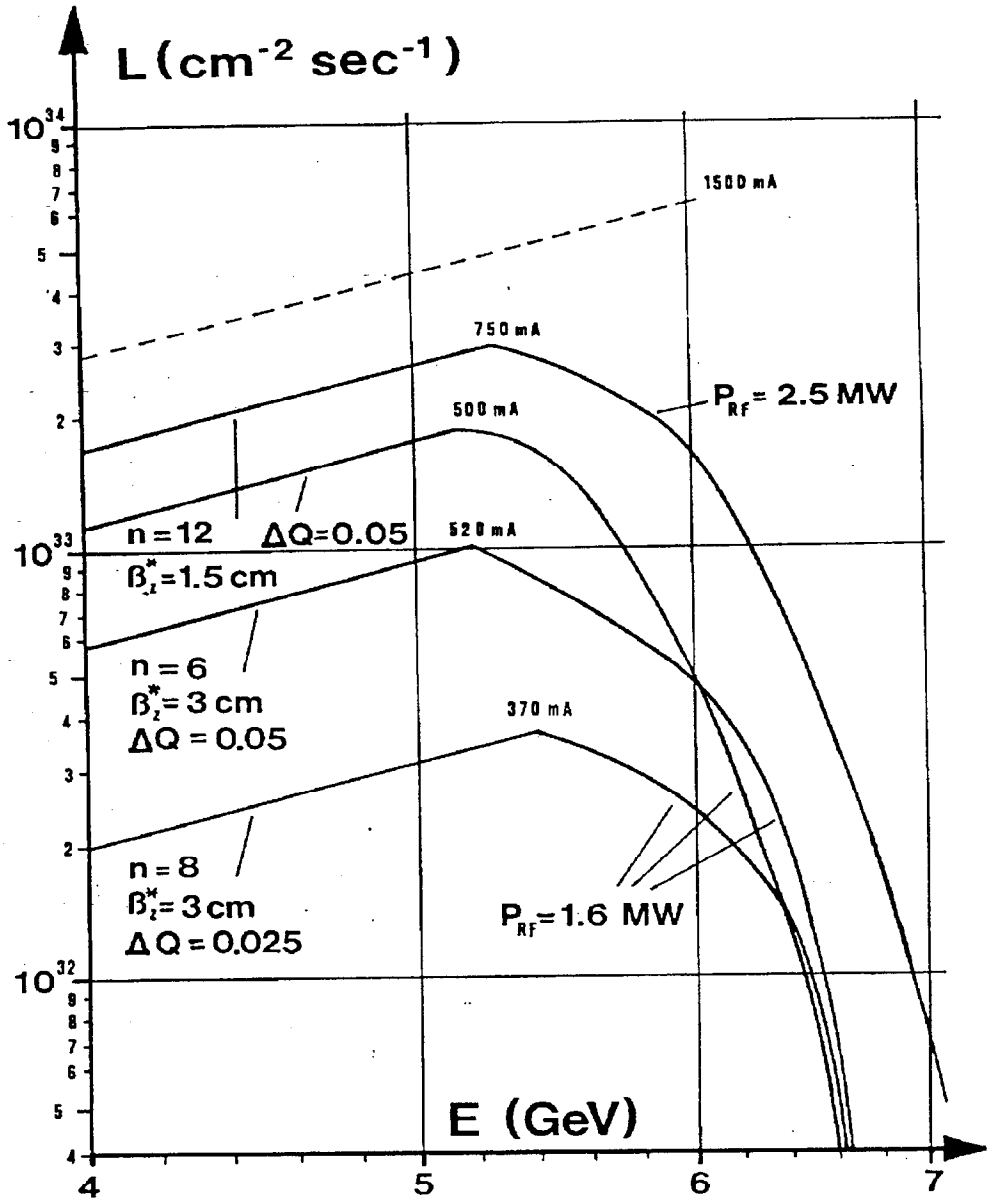

Figure 21. The design luminosity for the proposed SIN machine. Improvement of ℓ is expected in stages as more is learned and machine improvements are made. The bottom curve is expected within the first year of operation, with subsequently higher levels achieved as operating experiece is gained. Finally, with n = 12, $\Delta\nu$ = 0.05 ($\Delta Q \equiv \Delta\nu$), $\beta^*_y (\equiv \beta^*_z)$ = 1.5 cm, and I_{beam} = 0.75A, $\ell_{peak} \sim 3 \times 10^{33}\,cm^{-2}sec^{-1}$ is projected.

ity the SBF is a candidate design. Table 5 gives some parameters of the SBF_0 and SBF. At E_b = 12.5 GeV, $\ell_{peak} \sim 10^{33}$ is projected for the SBF_0, and $\ell_{peak} \sim 6 \times 10^{33}$ for the SBF. The large rf power required for the SBF and perhaps the SBF_0 as well, may demand the use of LEP type klystrons and superconducting cavities. The klystrons are now "off the shelf" items obtained from Philips (Cat. #YK1350), are rated for 1 MW output power, and have a central frequency of 352.21 MHz, the PEP rf frequency. Figure 22 shows a schematic of the Philips tube. In addition, superconducting cavities at the same frequency should also be available from European industrial sources in a couple of years (as a small add on order to LEP's).

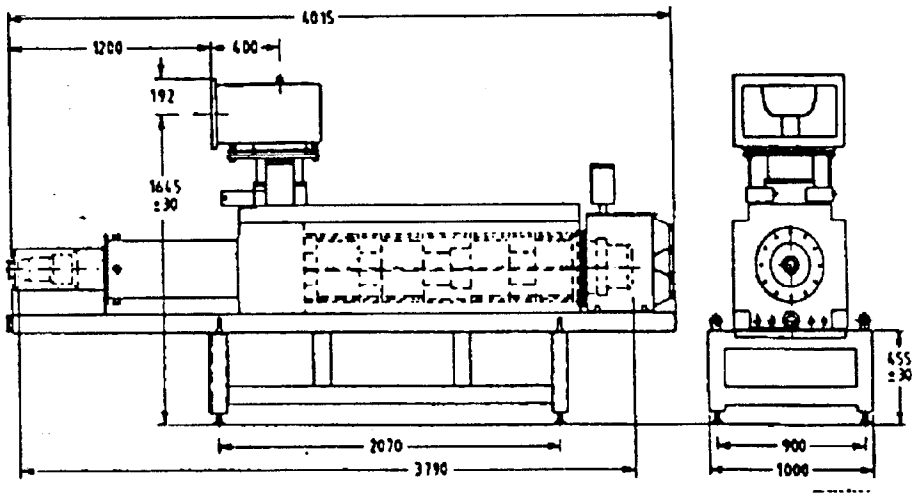

Figure 22. Philips YK 1350 continuous-wave high-power klystron. Water cooled, high efficiency, fixed frequency (353.31 MHz), 1 MW klystron in metal-ceramic construction. Cost per klystron is ~ $1m installed with power supply. Dimensions in the figure are in cm.

CONCLUSIONS

The chance to gain insight into a possible new mass scale plus many other physics opportunities that a sample of 10^7 B-decays brings is a physics justification for a B-factory by itself. Proton machines can produce this number of B's in the near future; however, detection efficiency presently severely limits this option. A really good trigger may make this approach practical. As for the e^+e^- colliders, linear collider designs all project interesting ℓ yielding ~10^7 B's/year, with some wisely allowing for boosted $\Upsilon(4S)$ production. However, all the designs contain very "high tech" elements

Table 5. Parameters for e^+e^- storage rings based on improvements to PEP. The present HiLum PEP is compared to the SBF_0 and SBF. The parameters discussed in the text are used to calculate projected performance.

	HiLum PEP	SBF_0	SBF
circumference(m)	2200	2200	2200
#rings	1	1	2
#IR'S	1	1	1
n	3	15	70
β^*_y	4	3	3
$\Delta\nu$	0.07 (@12.5)	0.08	0.08
Wigglers	no	yes	yes
L_{peak} ($\times 10^{32}$ cm^{-2} sec^{-1})			
@12.5 GeV/beam	1.4	13.2	61.6
@5.4 GeV Υ(4S)	NA	2.4	11.1
<L> (pb^{-1}/day)			
@12.5 GeV/beam	4.0	38.0	177.3
@5.4 GeV Υ(4S)	NA	6.8	31.9
P_{beam} (MW)			
@12.5 GeV	0.3	4.0	18.8
@5.4 GeV Υ(4S)	NA	0.7	3.4
I_{bunch} (ma)			
@12.5 GeV	8.3	11.9	11.9
@5.4 GeV Υ(4S)	NA	5.1	5.1
I_{beam} (ma)			
@ 12.5 GeV	24.9	178.9	834.9
@5.4 GeV Υ(4S)	NA	75.9	354.0
$B\bar{B}$ pairs/200 days ($\times 10^6$)			
@ 12.5 GeV	0.04	0.35	1.6
@5.4 GeV Υ(4S)	NA	1.4	6.4

which place such machines in the far future at best. The storage ring machines discussed in this paper all can produce ~ few times 10^6 B-decays or more in a reasonable running time; however, the SIN design (and CESR as well) which optimizes the machine for symmetric beams with E_{cm} at the Υ(4S) does not allow for measurements of B-lifetime, and so a crucial window on CP violation is lost. The SBF concept may

be just sufficient to achieve a measurement of CP violation in the B-system, but the development of such a machine and the measurements will probably require a staged effort (SBF_0) over a decade.

An e^+e^- machine, has an additional benifit. Beside prolific B-meson production it will yield more than 10^7 τ-lepton and C-meson and baryon decays while the B's are being produced. Thus many questions involving heavy flavor physics can be addressed at such a facility.

It is clear that much development work is needed in both the machine physics and detector design to achieve the CP violation measurement goals. It seems prudent to start in earnest soon, and to expect an extended effort.

ACKNOWLEDGEMENTS

Many of my colleagues have contributed to the content of this report. There are a number of major areas that I would like to separately acknowledge. First, my motivation to pursue this nascent field of CP violation in the B-system was sparked by extensive conversations with I. Bigi (SLAC), A. Fridman (CERN/SLAC/UCLA), F. Gilman (SLAC), H. Harari (Weizmann/SLAC), and P. Oddone (LBL). These colleagues have also suggested examples to clarify the physics goals, a number of which I have used in this report. Second, the section on "Where to B" was packed with the work of W. Hofmann (Berkeley) and G. Wormser (SLAC), as the section on linear colliders was packed with the work of P. Wilson (SLAC). Finally, the genesis of the SBF machine concepts have been strongly influenced through many discussions with M. Donald and D. Ritson of SLAC. In addition, important contributions to these ideas have been made by many members of the SLAC accelerator physics group, and H. Nesemann (DESY), D. Rubin (Cornell), R. Siemann (Cornell), R. Talman (Cornell), K. Wille (Dortmund), and H. Wiedemann (SSRL). Finally, I would like to thank L. Friedsam, G. Godfrey and P. Grossewiesmann (SLAC) for a careful reading of the manuscript.

REFERENCES

1. H. Albrecht, et al., (ARGUS), Phys. Lett. 192B, 247(1987).

2. For example see: I.I. Bigi and A. Soni, Phys. Rev. Lett. 53, 1407(1984); I.I. Bigi and A.I. Sanda, Phys. Rev. D29, 1393(1984).

3. J.S. Hagelen, Phys. Rev. D20, 2893(1979).

4. For a recent review see the talks of: A. Montag, D. Muller, and R. Ong, Proceedings of the 2nd International Symposium on the Production and Decay of Heavy Flavors, Stanford University Stanford, CA, Sept. 1–5, 1987, proceedings edited by E.D. Bloom and A. Fridman, (1988).

5. I.I. Bigi and A.I. Sanda, SLAC-PUB-4299, (1987).

6. I. Wingerter (UA-1), Proceedings of the 2nd International Symposium on the Production and Decay of Heavy Flavors, Stanford University, Stanford, CA, Sept. 1–5, 1987, proceedings edited by E.D. Bloom and A. Fridman, (1988).

7. B. Winstein, Proceedings of the Fourteenth SLAC Summer Institute on Particle Physics, SLAC Report No. 312, 33(1987).

8. H. Harari, Proceedings of the Twelfth SLAC Summer School on Particle Physics, SLAC Report No. 281, 264(1985).

9. R.N. Mohapatra and G. Senjanovic, Phys. Rev. Lett. 44, 912(1980); Phys. Rev. D23, 165(1(81). See also, H. Harari, Proceedings of the Fourteenth SLAC Summer School on Particle Physics, SLAC Report No. 312, 1(1987).

10. Much effort has gone into these questions at past conferences and workshops. Below is a partial list:
-- Workshop on e^+e^- Physics at High Luminosities, SLAC Report No. 283, proceedings edited by H. Paar, (1985);
-- 1st International Symposium on the Production and Decay of Heavy Flavors, University of Heidelberg, Heidelberg, FRG, May 20–23, 1986,

proceedings edited by K.R. Schubert and R. Waldi, DESY report (1986);
-- Critical Issues in the Development of New Linear Colliders, University of Wisconson, Madison, WI, Aug. 27–29, 1986, AIP Proceedings 156, 413-452(1987);
-- The Linear-Collider BB Factory Conceptual Design Workshop, University of California, Los Angeles, CA, Jan. 26–30, 1987, proceedings edited by Donald H. Stork, World Scientific (1988);
-- 2nd International Symposium on the Production and Decay of Heavy Flavors, Stanford University, Stanford, CA, Sept. 1–5, 1987, proceedings edited by E.D. Bloom and A. Fridman, New York Academy of Sciences, (1988);
-- B-Meson Factory Workshop, SLAC, Stanford University, Sept. 7–8, 1987, proceedings edited by L. Friedsam, SLAC Report 324, (1988).

11. B. Cox, proceedings of the B-Meson Factory Workshop, SLAC, Stanford University, Sept. 7–8, 1987, proceedings edited by L. Friedsam, SLAC Report 324, (1988).

12. I.I. Bigi and A.I. Sanda, Nucl. Phys. 281, 41(1987); also, Ref. 5.

13. Figure 6 is essentially from the talk of P. Oddone presented at The Linear-Collider BB-Factory Conceptual Design Workshop, University of California, Los Angeles, CA, Jan. 26–30, 1987, proceedings edited by Donald H. Stork, World Scientific 423(1988). Oddone discussed both symmeteric and asymmetric colliders and their interaction with potential detectors.

14. W. Hofmann, et al., Workshop on e^+e^- Physics at High Luminosities, proceedings edited by H. Paar, SLAC Report No. 283, 35(1985).

15. T. Sjoestrand, Comm. Phys. Comm. 27, 243(1982); 28, 229(1983). This relatively early version of the Lund Monte Carlo was tuned by W. Hofmann to match the available data for heavy quark processes.

16. W. Hofmann, Private communication. This work used Lund V6.3 with the Peterson Fragmentation function and $\epsilon_b = 0.01$. The accuracy of this model is

discussed in, J. Chrin, Proceedings of the 2nd International Symposium on the Production and Decay of Heavy Flavors, Stanford University, Stanford, CA, Sept. 1–5, 1987, proceedings edited by E.D. Bloom and A. Fridman, New York Academy of Sciences, (1988).

17. H. Airara, et al., (TPC/2γ), Phys. Lett. B 134, 299(1987).

18. G. Wormser, MarkII/SLC — Physics Working Group Note #9-15, (1987). This work has been submitted for publication, see G. Wormser, et al. (Mark II), SLAC-Pub-4536 (1988).

19. P. Wilson, Proceedings of the Linear Collider BB-Factory conceptual Design Workshop, editor: D. Stork, World Scientific, 373(1987); and, SLAC-PUB-4310(1987). This section on linear colliders borrows heavily from these references.

20. R. Hollebeek, Nucl. Inst. Meth. 184, 333(1981); W. Fowley and E. Lee, CERN 87-11, ECFA 871110, VOL II, 605(1987). Figure 11, showing the result of the calculations, was taken from D. Cline, UCLA Center for Advanced Accelerators-1, (1988).

21. U. Amaldi and G. Coignet, Nucl. Instr. Meth. A260, 7(1987).

22. J. S. Wurtele and A. M. Sessler, TBA Note 33, Lawrence Berkeley Laboratory, (1986).

23. D. Cline, Proceedings of the Linear Collider BB-Factory Conceptual Design Workshop, editor: D. Stork, World Scientific, 386(1987).

24. E. Eichler, et al., Motivation and Design Study for a B-Meson Factory with High Luminosity, SIN-PR-86-13, (1986).

25. K. Berkelman, proceedings of the B-Meson Factory Workshop, SLAC, Stanford University, Sept. 7–8, 1987, proceedings edited by L. Friedsam, SLAC Report 324, (1988).

26. J.M. Paterson, et al., PEP Note 125, (1975).

27. J.T. Seeman, SLAC-PUB-3825, (1985).

28. R.H. Siemann and R. Talman, Private Communication.

29. H. Wiedemann, Proceedings of the Workshop on PEP as a Synchrotron Radiation Source, SLAC, Stanford University, Oct. 20–21, 1987, SSRL Report, 18(1987).

30. K.-Wille, Proceedings of the B-Meson Factory Workshop, SLAC, Stanford University, Sept. 7–8, 1987, proceedings edited by L. Friedsam, SLAC Report 324, (1988); and Proceedings of the 2nd International Symposium on the Production and Decay of Heavy Flavors, Stanford University, Stanford, CA, Sept. 1–5, 1987, proceedings edited by E.D. Bloom and A. Fridman, New York Academy of Sciences, (1988).

31. M. Sands, SLAC-PUB 121, Eq. 5.85, (1970).